

# Flow Indices Variability in Humid Subtropical of Upper Awash River Basin, Ethiopia

Sintayehu Yadete Tola (✉ [sintayadete5@gmail.com](mailto:sintayadete5@gmail.com))

National Institute of Technology Karnataka

Amba Shetty

Department of Water Resources and Ocean Engineering, National Institute of Technology Karnataka

---

## Research Article

**Keywords:** Variability, Discharge, modified MK test, ITA

**Posted Date:** December 15th, 2021

**DOI:** <https://doi.org/10.21203/rs.3.rs-908354/v1>

**License:**   This work is licensed under a Creative Commons Attribution 4.0 International License.

[Read Full License](#)

---

# 1 **Flow Indices Variability in Humid Subtropical of Upper Awash River Basin, Ethiopia**

2 Sintayehu Yadete Tola<sup>1</sup> and Amba Shetty<sup>2</sup>

3 <sup>1\*</sup> Department of Water Supply and Environmental Engineering, Arba Minch Water Technology Institute, Arba  
4 Minch University PO. Box 21, Arba Minch, Ethiopia. Department Water Resources and Ocean Engineering,  
5 National Institute of Technology Karnataka, Srinivasnagar Surathkal, Mangalore, Karnataka, 575025, India.

6 \*Corresponding Author: [sintayadete5@gmail.com](mailto:sintayadete5@gmail.com)

7 <sup>2</sup>Department of Water Resources and Ocean Engineering, National Institute of Technology Karnataka,  
8 Srinivasnagar Surathkal, Mangalore, Karnataka, 575025, India.

9 E-mail: [amba\\_shetty@yahoo.co.in](mailto:amba_shetty@yahoo.co.in)

## 11 **Abstract**

12 Investigating the hydrological extremes indices at high resolutions describing the whole stream spectrum is  
13 essential for the comprehensive assessment of watershed hydrology. The study focuses on a wide-ranging  
14 assessment of river discharge in annual mean, peak, and high and low percentiles flow at the Upper Awash River  
15 basin, Ethiopia. Statistical tests such as coefficient of variation, flood variability to characterize the flow regime  
16 and Tukey's test to detect decadal variability. Modified Mann-Kendall test, Sen's slope estimator, innovative  
17 trend analysis and Pettitt's test were applied to see trends, and change points in time series, respectively. Results  
18 showed that the basin was characterized by moderate to high variability. Spatially, main tributaries showed a  
19 higher variability, almost in all-time step and characterized by higher flood variability. The large discharge  
20 receiving rivers resulted in a moderate to high and lower discharge variability. Test statistics resulted in a positive  
21 increasing trend dominating most time scales at a 5% significant level and higher magnitude of slope trend in  
22 peak flow. A negative trends were also exhibited. Hombole main outlet site experienced decreasing trend in high  
23 percentile flow. In comparison, complete trend direction agreements were observed (except in few series). Flow  
24 indices showed an upward shift and downward shift mainly in the year 2000s and the significant decadal variation  
25 resulted in comparable with change points. The study provides an understanding of water resources variability,  
26 which will be necessary to apply operational water resources strategies and management to restrain the potential  
27 impacts of variability nature of the streamflow.

28 Key Words: Variability, Discharge, modified MK test, ITA

## 29 **1 Introduction**

30 Water resource management is a severe issue for sustaining the environment due to its variability. It is generally  
31 understood that the chain reaction of climate variability and land use land cover change impacted the  
32 hydrological cycle components (Legesse et al. 2003, 2010; Bao et al. 2019; Liu et al. 2020). In the first instance  
33 mainly, extreme hydrological events such as floods and droughts are of consequences (IPCC 2014). Climate  
34 change impact on streamflow is extensively studied. In particular, precipitation and temperature change are  
35 sensitive to change in streamflow characteristics (Hailemariam 1999; Jha et al. 2004; Guo et al. 2008;  
36 WaleWorqlul et al. 2018; Nilawar and Waikar 2019; Vandana et al. 2019) at basin and at global scale (Palmer  
37 et al. 2008). On the other hand, due to increased human-induced land cover change, such as noticeable  
38 urbanization, cropland expansion, deforestation, population growth, etc., the sub/terrestrial hydrological process  
39 have been affected (Nie et al. 2011; Billi et al. 2013; Shawul et al. 2019). Thus, climate change is not the only  
40 the causer of hydrological regime change. However, the discharge of the rivers is of significant implications in  
41 parts of extensively developed and center of socioeconomic undertakings for future water resources availability,  
42 water resource planning, and flood discharge management.

43 The topographic, climatic characteristics and recent anthropogenic activities have made the rivers  
44 vulnerable to varying discharges and Awash River basin is no exception to it. The river basin is the most  
45 exploited basin for agriculture (irrigation and rainfed agriculture) and the center of socioeconomic activities.  
46 The basin experienced frequent extreme hydrological (i.e., riverine floods and flash floods), and climatological  
47 hazards in the past 3 to 4 decades (Edossa et al. 2010; Belayneh et al. 2014). The dense population with  
48 urbanization in the region, water supply, irrigation, and hydroelectric dams, are dependent on the rivers  
49 originating in the upper land, including the capital city of Addis Ababa, and Adama town. In particular, the  
50 Upper basin has undergone an extensive land cover change (Shawul and Chakma 2019; Tadese et al. 2020b)  
51 over the past 3-4 decades and indicated the impacts on hydrological cycle variables (Shawul et al. 2019; Tadese  
52 et al. 2020a). However, extreme discharges in response to land cover change are more pronounced in small-  
53 scale watersheds (Blöschl et al. 2007; Apollonio et al. 2016).

54 In order to explore hydrological change and variation, identifying a trend and probable change point is a  
55 robust inference toward local climate change and anthropogenic activities (Gebremicael et al. 2017; Belihu et  
56 al. 2018). It is worth mentioning several factors that affect river flow discharge such as reservoir operation,  
57 water diversion, water withdrawal, irrigation scheme, implementation of flood control structures etc. With

58 global warming, intensification of hydrological cycle expected to continue into the future and directly manifests  
59 in a pronounced way in extreme hydrological conditions, i.e., flooding and water availability (Asadieh and  
60 Krakauer 2017; Tabari 2020). Moreover, observed extreme flow is considerably vital in water resource  
61 management and climate and anthropogenic activity assessments. Numerous hydroclimatic metrics are available  
62 in literature to detect trends in average, annual, monthly, seasonal, extreme (high and low) resolutions for better  
63 hydroclimatic insight in detail (Bekele et al. 2017; Gudmundsson et al. 2018; Ruwangika et al. 2020). Peak-  
64 over-threshold approaches is also alternative to annual maximum flow often associated with flood frequency  
65 analysis.

66 Several studies have been carried out in Ethiopia, focusing on hydroclimatic trends at catchment scale  
67 (Belihu et al. 2018; Orke and Li 2021) and basin scale (Tekleab et al. 2013; Jaweso et al. 2019). Hydroclimatic  
68 variability is the primary concern in the basin to water resource availability, especially in Awash River basin  
69 (Bekele et al. 2017; Taye et al. 2018; Daba and You 2020). Recent trend studies carried out by Gedefaw et al.  
70 (2018), Tadese et al. (2019) and Daba et al. (2020) used annual and seasonal time scale in the Upper Awash  
71 River basin hydrometric station. Daba et al. (2020) reported no trends in annual and seasonal (Kiremt and Belg)  
72 discharges and Bega season showed significant trends at two stations. They indicated increasing discharges were  
73 abundant in the Upper Awash basin. Tadese et al. (2019) applied trend test over Awash River basin annual and  
74 seasonal steps, and increasing trends were observed predominantly. Gedefaw et al. (2018) concluded a  
75 decreasing trend of annual discharge in Upper Awash River flow on the basis of the average flow of four stations.  
76 Although, at main river outlet, for instance, Hombole station conflicting trend results were reflected on the  
77 annual scale. These studies focused on detecting the homogeneity tests and trends in hydroclimatic variables  
78 using commonly MK test and Sen's slope estimator at courser time scales. Long-term hydroclimatic evaluation  
79 alone cannot be satisfactory in understanding the pattern characteristics of temporal variations and it is important  
80 to examine at different time scales. It has the advantage of defining the entire range of flows observed each year.  
81 Moreover, water managers are interested in flood and drought assessment in a basin like Awash River basin  
82 where surface flow availability depends on precipitation for rainfed and agricultural irrigation as the backbone  
83 of the economy and food security. In this case, though there have been studies on long-term streamflow  
84 variability in the river basin under investigation, and it could not describe the high-resolution variations.  
85 Investigating the hydrological extremes indices at high resolutions describing the whole stream spectrum is  
86 essential for the comprehensive assessment of watershed hydrology.

87 Several studies have been carried out using statistical test methodologies to measure the significant changes  
88 in time series. Parametric and non-parametric tests have been used to identify the presence of significant trends  
89 in hydroclimatological studies (Partal and Kahya 2006; Wilson et al. 2010; Jaiswal et al. 2015; Meresa et al.  
90 2017; Drissia et al. 2019). Other recent trend analysis tools are based on time frequency, such as wavelet  
91 transformation (continuous and discrete wavelet transform), but the complex analyses (Ruwangika et al. 2020).  
92 Hydrological data are mostly not normally distributed. Compared to the parametric test (linear regression), the  
93 non-parametric test (Mann-Kendall, Sen's slope, Spearman rho test, etc.) has no prerequisite assumptions of  
94 distribution of the data series and is preferably robust to non-normally distributed data series and outliers. Many  
95 studies have widely used a rank based non-parametric Mann-Kendall (MK) test (Petrow and Merz 2009; Degefu  
96 et al. 2019; Jaweso et al. 2019) and Pettitt's test (Arrieta-Castro et al. 2020; Ryberg et al. 2020) for trend and  
97 change point detection in hydroclimatic data series, respectively. The MK test, however requires the serial  
98 independence of data time series. Innovative trend analysis (ITA) was developed by Şen (2012). In most recent  
99 ITA has been widely used to detect trends in annual and seasonal rainfall (Wu and Qian 2017; Caloiero et al.  
100 2018; Gedefaw et al. 2018; Wang et al. 2020), monthly total precipitation (Ay and Kisi 2015), annual  
101 temperature (Gedefaw et al. 2018), pan evaporation (Kisi 2015), Solar radiation (Zhou et al. 2018) in different  
102 areas of the world. In hydrological variables, Kuriqi et al. (2020) applied MK test, Sen's slope estimator and  
103 ITA to assess trends in Godavari River basin of India for monthly, annual mean, annual maximum and minimum  
104 flow and seasonal time scales. ITA has been compared with MK, Sen's slope estimator, linear regression and  
105 Spearman's Rho test in all these studies. It is superior to detect sub-trends in data series from graph plots,  
106 independent of the statistical distribution and autocorrelation assumptions and sample size. MK test coupled  
107 with Sen's slope and ITA is demonstrated to be exceedingly effectual in detecting both quantitative and  
108 qualitative trend analyses.

109 Moreover, the evidence obtained from such analysis is vital in developing a compressive plan and mitigation  
110 approaches at basin scale. The long-term river discharge trend, especially the extreme hydrological events, are  
111 preconditions in the basin where flood results loss to the lives and crops. For this reason, it is needed to use a  
112 high resolution of stream data to detect trends in tributaries and main river sections to identify hydrological  
113 behaviour in the regions. Therefore, systematic evaluation of hydrological indices that capture the critical  
114 aspects such as decadal, mean annual, peak flow and flow percentiles yearly time step (99<sup>th</sup>, 95<sup>th</sup>, 90<sup>th</sup>, 10<sup>th</sup>, 5<sup>th</sup>,  
115 and 1<sup>st</sup>) indices of streamflow evident the understandings availability of water resources and sustainability of  
116 the ecosystem in river basin. Moreover, underlying the significant change detection of hydrological indices is

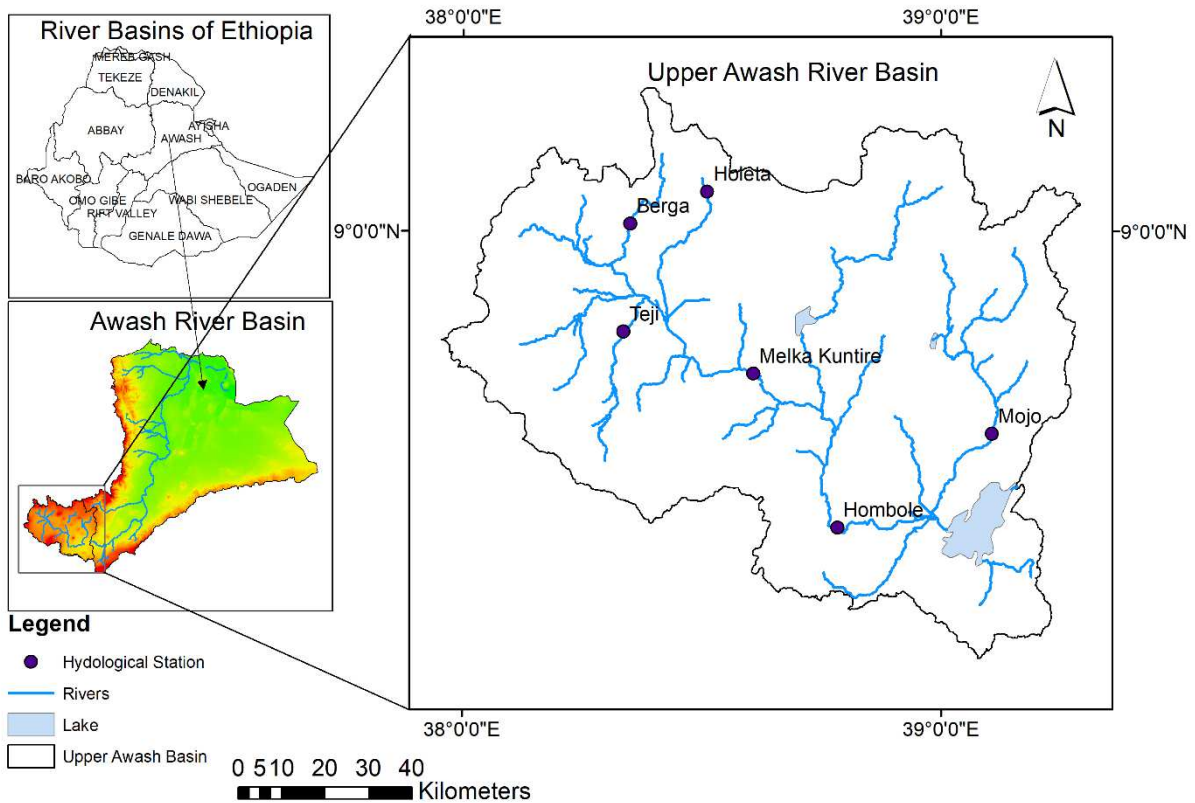
117 particularly important to understand the increasing concern of the collective effect of climate changes and human  
118 activities on hydrological responses. The result has more comprehensive practical application to integrated water  
119 resources management and adaptation measures. Hence, the study aims to investigate the discharge variability,  
120 detect significant trends, and change-point in long-term hydrological indices of the Upper Awash River basin.

## 121 **2 Materials and Methods**

### 122 **2.1 Study Area and Data Sets**

123 The study was conducted in Upper Awash River basin (UARB) bounded between 8<sup>01</sup>' and 9<sup>04</sup>' latitude and  
124 37<sup>058</sup>' and 39<sup>04</sup>' longitude Fig. 1. The mean annual precipitation over the regions is 1030 mm (Daba et al. 2020)  
125 and higher (Mulugeta et al. 2019). Unimodal rainfall distribution (Edossa et al. 2010) and humid subtropical  
126 highland according to Köppen climate classification zones of Ethiopia. Awash basin is characterized by variable  
127 climate conditions resulting in frequent floods and droughts.

128 The Digital Elevation Model of the Awash basin ranges from 4195 to 240 masl (meter above sea level) and  
129 Upper Awash elevation covers above 1500 masl. The Awash River originates at the highland of Ethiopia Ginchi  
130 at an elevation between 2400 and 2900 masl in the Western and flows through high plateaux to north eastward.  
131 The study region is the strategic source of water resources. The majority of the population are living on the  
132 highland areas, above 1500 amsl. Due to the climatic condition, soil fertility, and suitability for agriculture, the  
133 regions are under intense pressure compared to others downstream. The upper highland areas are composed of  
134 high plateaux, high to mountainous relief hills, and dissected plateaux with hills plain. Rapid population  
135 increment and urbanization predominantly modified the land-use system in the upper basin.



136

137 **Fig. 1** River basin of Ethiopia, digital elevation model of Awash River Basin, UARB stream networks, lake,  
 138 and hydrological stations

139 Long historical daily streamflow data were obtained from the hydrology department, Ethiopian Ministry of  
 140 Water, Irrigation and Energy. Sets of representative gauging stations (Fig. 1), Holeta, Berga Teji, Melka  
 141 Kunture, Hombole and Mojo are selected for the current study from upper to lower reach based on the data  
 142 availability. Table 1 presents the catchment area of the stations, data sets of the diverse periods and the  
 143 percentage of missing data series, which were filled later using linear regression techniques. The selected  
 144 stations have a maximum of 48 years of observations and have at least 35 years. The spatial stations are clustered:  
 145 upper reach includes four stations (Holeta, Berga, and Teji), middle consists of one station (Melka Kunture) and  
 146 lower space include two stations (Hombole and Mojo).

147

148

149

150

151

152

153

**Table 1** Data sets: list of stations, area, period of record and percentage of missing data

Stations	Area (km <sup>2</sup> )	Period of record	Percentage of missing
Holeta	199	1975-2009	5.4
Berga	248	1975-2012	4.04
Teji	662.5	1980-2014	8.1
Melka Kunture	4456	1965-2012	1.77
Hombole	7656	1968-2014	0
Mojo	1264.4	1970-2014	5.2

154

155

The annual mean, annual peak flow, and percentiles flow of 99<sup>th</sup>, 95<sup>th</sup>, 90<sup>th</sup> defined as the high flow and low flow as 10<sup>th</sup>, 5<sup>th</sup>, and 1<sup>st</sup> were extracted for analysis from daily data series. Considering large sets of hydrological variables enables us to explore the broader impacts of the climate and anthropogenic on watershed hydrology.

156

157

## 158 **2.2 Statistical Analysis**

159

In order to provide the existence of healthy hydrological characteristics over the historical period, coefficient of variation and discharge variability index were used in this study to explore further variability in hydrological indices. The statistics of coefficient variation (CV) is the ratio of standard deviation to mean. This study employed coefficient of variance to summarize streamflow variation degree to mean streamflow record periods of annual mean, annual peak and percentile flows and determine the significant level of variation in the data structures. CV has been applied in the long term hydroclimatic variability studies (Chen et al. 2014; Kisaka et al. 2015). For the present study the fundamental statistics CV values were defined as normal (<0.2), moderate (0.2 - 0.3), and highly variable (> 0.3) to periods of records (Tadese et al. 2019). Flood discharge variability index (maximum discharge divided by the annual mean discharge,  $Q_{max}/Q_{mean}$ ) were used in this study to characterize the hydrological regime characteristics in the watershed. The indices were demonstrated in river discharge behavior (Hansford et al. 2020) study over 575 gaging stations in response to different climatic zones, including the humid subtropical climate type.

160

161

162

163

164

165

166

167

168

169

170

171

In addition, Tukey's HSD (honestly significant difference) multiple comparison test was used to evaluate the pattern of difference between means. Before Tukey's HSD test, if the analysis of variance among the groups of means is significant, it means at least one group differs from the other groups, and detail can be referred from Williams and Abdi (2010). Tukey's test at a decadal resolution of the annual mean flow, peak flow, 95<sup>th</sup> and 10<sup>th</sup> percentile flows was applied to test the mean variability. The time interval was selected from 1970-1979, 1980-1989, 1990-1999, and 2000-2009. All pairwise differences were evaluated using the same sample size

172

173

174

175

176

177 used for the most significant difference. The null hypothesis assumed that there was no significant difference  
 178 between means and the alternative hypothesis was assumed that a significant difference exists in means at a 5%  
 179 significance level. The Tukey's HSD approach has been applied to test the hydrological variation in decadal  
 180 resolution in Lake Tana Basin, Ethiopia (Tigabu et al. 2020).

## 181 **2.3 Trend Analysis Methods**

### 182 **2.3.1 Mann-Kendall Trend Test (MK)**

183 In the current study, a robust non-parametric MK trend test (Mann 1945a; Kendall 1975) method was applied  
 184 to detect trends in the hydrological time series. MK test, however, requires the serial independence of data time  
 185 series. The existence of serial correlation leads to the rejection of the null hypothesis (no trend) and accepts the  
 186 significant trend (Von Storch and Navarra 1995). The procedure for MK tests starts with statistic (S), and is  
 187 given by Eq. (1).

$$Sgn = \sum_{i=1}^{n-1} \sum_{j=i+1}^n Sgn(X_j - X_i) \quad (1)$$

188 Where  $X_j$  and  $X_i$  are consecutive observations data and  $n$  is the length of the data series. The  $Sgn(X_j - X_i)$  is set  
 189 as,

$$Sgn(X_j - X_i) = \begin{cases} +1 & X_j - X_i > 0 \\ 0 & \text{if } X_j - X_i = 0 \\ -1 & X_j - X_i < 0 \end{cases} \quad (2)$$

190 The data series variance  $Var(S)$  was estimated by:

$$Var(S) = \frac{n(n-1)(2n+5) - \sum_{i=1}^q t_i(t_i-1)(2t_i+5)}{18} \quad (3)$$

191 Where,  $n$  is the length of observations,  $q$  is the number of pairs observation in data series,  $t_i$  is the number of  
 192 pairs observations in series at the time  $i$ .

193 Finally, the standard Z statistics value was calculated by:

$$Z = \begin{cases} \frac{S-1}{\sqrt{\text{Var}(S)}} & S > 0 \\ 0 & \text{if } S = 0 \\ \frac{S+1}{\sqrt{\text{Var}(S)}} & S < 0 \end{cases} \quad (4)$$

194

195 The  $Z$  value determines the existence of increasing, decreasing, and no trend in time series. When  $Z$  value  
 196 is greater than zero, it indicates the increasing trend, and a negative value suggests decreasing trend. The critical  
 197 value at a two-tailed 1%, 5%, 10% significant level is  $\pm 2.576$ ,  $\pm 1.96$  and  $\pm 1.645$ . In this study, 5% significant  
 198 level was used to detect the trend and a significant increase or decrease is accepted if the  $Z > \pm 1.96$  (Diop et  
 199 al. 2017)

### 200 **2.3.2 Modified Mann-Kendall Trend Test (MMK)**

201 The existence of serial correlation leads to the rejection of the null hypothesis (no trend) and accepts the  
 202 significant trend (Von Storch and Navarra 1995). Mann-Kendall test (Mann 1945b; Kendall 1975) do not  
 203 consider the lag-1 autocorrelation in hydrological time series. Before test was performed, the Ljung-Box serial  
 204 autocorrelation test (Ljung and Box 1978) was used to assess individual variables. For  $N$ , serially correlated  
 205 observations contain the same information as  $N^* < N$  (lower than original series size). In the presence of positive  
 206 (negative) serial correlation, the variance ( $S$ ) of MK test is fluctuating (increase or decrease). Thus for this study  
 207 modified Mann-Kendall test for serially correlated data using the Yue and Wang (2004) variance correction  
 208 approach was used to reduce the effect of serial correlation and the corrected variance  $S$  of MK test is given as;

$$V(S)_{cor.} = CF * V(S) \quad (5)$$

209 Where  $V(S)_{cor.}$  is corrected variance,  $V(S)$  is the original variance of sample and  $CF$  is correction  
 210 factor. Yue and Wang (2004) introduced the correction factor  $CF$  expressed as follow;

$$CF = 1 + 2 \sum_{k=1}^{N-1} (1 - K / N) r_k \quad (6)$$

211 Where  $r_k$  is the lag- $k$  serial correlation of the observed serial and  $N$  is the total length of the data series.  
 212 Variance correction approach has been used to correct the serial correlated hydrological series data by many  
 213 latest studies and detected the trend to corrected variance (Wang et al. 2015; Azam et al. 2018). The test was  
 214 applied for annual mean, peak and high and low percentile flows at lag-1 to detect trends in the flow indices.

### 215 2.3.3 Sen's Slope Estimator (SSE)

216 If a trend exists, the magnitude of linear trend slope in time series is estimated using a non-parametric approach  
217 (Theil, 1950 and Sen, 1968). Monotonic trend slope was calculated using:

$$\alpha_i = \text{Median} \frac{X_i - X_j}{i - j} \forall i \geq j \quad (7)$$

218  $x_i$  and  $x_j$  are the data observation corresponding to time  $i$  and  $j$ . The median of  $N = n(n - 1)/2$  for  $\alpha_i$  is  
219 Sen's estimator of the slope where  $n$  is the number of periods. The  $\alpha_i$  is tested against the two-sided test at 5%  
220 significant level and the actual slope is estimated by a non-parametric test. The sign of the  $\alpha_i$  obtains the  
221 increasing if  $\alpha_i$  is positive and decreasing if  $\alpha_i$  is negative.

### 222 2.3.4 Innovative Trend Analysis (ITA)

223 The ITA was first developed by (Şen 2012). The data time series is divided into two equal sub-series and ordered  
224 in ascending. The first half time-series sets are placed in the x-axis, and the second half time data sets are also  
225 placed in the y-axis in the Cartesian coordinate system. If the two sub-series are alike, the data points in the plot  
226 scatter show along the 1:1(45<sup>0</sup>) line, which divides into upper and lower triangles. Upper exhibits an increasing  
227 trend if the data points fall above the 1:1 line and if the data points found in the lower triangle, the series reveals  
228 decreasing trend and no trend along the 1:1 line (Şen 2012). Else, the scatter point present non-monotonic trend  
229 consisting of different trends in the time series categorized into cluster as low, medium and high cluster points.  
230 The ITA trend slope (S) is estimated by using the following expression (Şen 2017).

$$S = \frac{2(\bar{X}_j - \bar{X}_i)}{n} \quad (8)$$

231 Where  $\bar{X}_i$  and  $\bar{X}_j$  are the arithmetic average of the first and second half time series, respectively, and  $n$  is  
232 the data set length. The stochastic property of S is a function of the arithmetic mean of the first half and second  
233 half time series. As  $\bar{X}_i$  and  $\bar{X}_j$  are also stochastic variables, the first-moment order (expectations) of the slope  
234 trend can be obtained by taking the expectation of both sides:

$$E(S) = \frac{2}{n} [E(\bar{X}_j) - E(\bar{X}_i)] \quad (9)$$

235  
236 In case of no trend detection, the centroid point fall on the 1:1 line (45<sup>0</sup>), indicating that  $E(\bar{X}_i) = E(\bar{X}_j)$  and  
237 hence,  $E(S) = 0$ . Then again, the variance of the slope can be computed as  $\sigma_s^2 = E(S^2) - E^2(S)$ , which is

238 equal to the second-order moment of the slope variable. Since  $E(\bar{X}_i^2) = E(\bar{X}_j^2)$ , then the variance of slope  
 239 equation can be expressed as;

$$\sigma_S^2 = \frac{8}{n^2} [E(\bar{X}_j^2) - E(\bar{X}_j \bar{X}_i)] \quad (10)$$

240

241 The correlation coefficient of the two mean values in the stochastic process is expressed:

$$\rho_{\bar{X}_j \bar{X}_i} = \frac{E(\bar{X}_j \bar{X}_i) - E(\bar{X}_j)E(\bar{X}_i)}{\sigma_{\bar{X}_j \bar{X}_i}} \quad (11)$$

242

243 Substituting the correlation coefficient of the two mean numerator into Eq. (11) and considering  $\sigma_{\bar{X}_j} = \sigma_{\bar{X}_i} =$   
 244  $\sigma/\sqrt{n}$  gives the variance of the slope as follow:

$$\sigma_S^2 = \frac{8}{n^2} \frac{\sigma^2}{n} (1 - \rho_{\bar{X}_j \bar{X}_i}) \quad (12)$$

245

246 Where,  $\rho_{\bar{X}_j \bar{X}_i}$  is the correlation coefficient of the two mean values in the stochastic process, finally the standard  
 247 deviation of the slope is given:

$$\sigma_S = \frac{2\sqrt{2}}{n\sqrt{2}} \sigma \sqrt{1 - \rho_{\bar{X}_j \bar{X}_i}} \quad (13)$$

248

249 Therefore, the statistical significance of the innovative trend slope test can be achieved through a normal  
 250 (Gaussian) PDF with zero mean and standard deviation equal to  $\sigma_S$ . If at  $\alpha$  percent significance level, the  
 251 confidence limits of a standard normal PDF with zero mean and the standard deviation is  $S_{cri}$ , then the confidence  
 252 limits (CL) of the trend slope is obtained as:

$$CL_{(1-\alpha)} = 0 \pm S_{Cri} \sigma_S \quad (14)$$

253 Where  $\alpha$  denotes significance level and  $\sigma_S$  is the standard deviation of the slope. The null hypothesis,  $H_0$ ,  
 254 infers that there is not a significant trend if the calculated slope value,  $S$ , remains less than a critical value,  $S_{cri}$ .  
 255 Otherwise, an alternative hypothesis,  $H_a$ , is accepted when  $S > S_{cri}$ . In this study, 5% significance level was  
 256 used for the ITA approach to mean annual, peak, high and low percentile flows.

## 257 2.4 Change-point Analysis

258 A non-parametric Pettitt's test (Pettitt 1979) was used to detect the abrupt change in the middle of the data series.  
259 This test was chosen because it is free distribution testing, adaptation of the rank-based Mann-Whitney test and  
260 has the advantage of sensitivity to identify the exact time of step change is anonymous. The method was most  
261 widely used in hydrological and climatological data (Kundzewicz and Robson 2004; Jaweso et al. 2019; Daba  
262 et al. 2020). If the observed sequence  $X_1, X_2, X_3 \dots X_n$  has a change point at time  $t$  such that  $X_1, X_2, X_3 \dots X_t$  has  
263 distribution function  $f_1(x)$  which is different from the distribution function  $f_2(x)$  of the series  $X_{t+1}, X_{t+2}, X_{t+3}$   
264  $\dots, X_{t+n}$ . Then the non-parametric test statistics,

$$K_T = \text{Max} |U_{t,T}|, 1 \leq t \leq T \quad (15)$$

265 Where  $U_{t,T} = \sum_{i=1}^t \sum_{j=i+1}^T \text{sgn}(X_i - X_j)$ ,  $\text{sgn}(x) = 1$  if  $X > 0$ ,  $0$  if  $X = 0$ , and  $-1$  if  $X < 0$ . The confidence level  
266  $p$ , of the sample  $n$  length and its associated  $K$  statistics,

$$\rho = \exp\left(\frac{-K}{n^2 + n^3}\right) \quad (16)$$

267

268 In this study, the 5 % significance level was considered. The null hypothesis of change not exist is rejected  
269 if the  $p$  values is less the specified significance level ( $\alpha = 0.05$ ) and accept the alternative hypothesis, change  
270 exist in the data series. The constancy statistical properties (stationary) of the stream flow indices before and  
271 after change point was evaluated by plotting probability of exceedence against descending order of stream flow  
272 of two group (before and after) using Weibull plotting position (Rao and Hamed 2000),  $i/n + 1$ , where  $i$  is rank  
273 in ascending order and  $n$  is the number of observations. Probability of exceedence of 10%, 50% and 90% was  
274 chosen to compare the discharge both before and after change point.

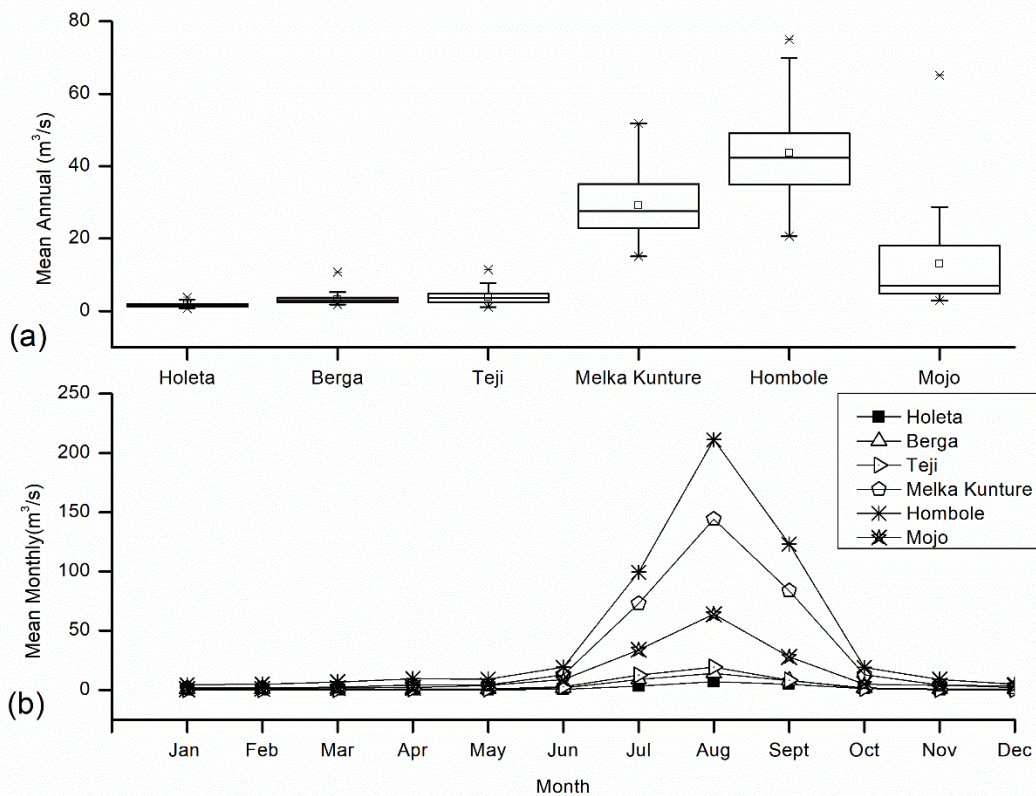
## 275 3 Results and Discussion

### 276 3.1.1 Spatial Variability of River Discharge

277 The highest mean annual discharge value was found to be in the lower reach of Hombole (43.66 m<sup>3</sup>/s) and the  
278 least in the upper Holeta (1.62 m<sup>3</sup>/s) hydrometric station. River discharges were confined to Kiremt (JJAS) and  
279 receive maximum precipitation in Kiremt season, but significant variation in runoff discharges could be

280 associated with catchments area and geomorphology. For instance, Hombole has the largest (7,656 km<sup>2</sup>) and  
281 Holeta (119 km<sup>2</sup>) has the smallest catchment area. The annual daily peak flow exhibited a high in the middle  
282 station of Melka Kunture (944.125 m<sup>3</sup>/s) in August and a lower reach of Hombole (803.10 m<sup>3</sup>/s). The daily  
283 discharge of Hombole and Melka Kunture stations had above zero minimum values while other stations had  
284 zero. The upper headwater station showed a maximum release of 45.95 m<sup>3</sup>/s at Holeta.

285 Main tributaries have shown almost the same mean annual flow in upper reach and the middle with lower.  
286 Stations along with the main river discharge accumulation are significantly increasing from Melka Kunture  
287 toward Hombole station. Spatially, the lower reach has the most extended duration and highest flow availability  
288 cover. On the other hand, stations in the middle and lower reach received higher average streamflow than upper  
289 reach. Compared to the other stations, the temporal flow distribution indicates that Hombole receives the highest  
290 flow annually. Middle reach obtained higher records as well. Holeta was the least to receive flow on annual  
291 scale. The flow in October may be attributed to the lesser flow difference between small rain and dry season in  
292 most stations, including Melka Kunture in middle and Hombole in lower. The most increased average monthly  
293 flow was presented in August, while July and September were moderate, and June and October lowest mean  
294 values during Kiremt (Fig. 2b). In addition, there was no significant dissimilarity in mean in all stations between  
295 October and June. Thus, the observed discharge value corresponds with the highest and tiny rainfall season.  
296 Over all spatial patterns of mean annual and mean monthly discharges are similar.



297

298 **Fig. 2** Long-term mean annual (a) and Monthly river discharges (b) of each station in UARB

299

300

301

302

303

304

305

306

307

308

309

310

311

The streamflow variability in mean annual flow, peak flow and percentiles flow was defined by the coefficient of variation (CV) statistics and is given in Table 2 and Table 3. Almost 66.6% of the station have shown high ( $> 0.3$ ) variability in mean annual and peak flow series, respectively. Remarkably, as far flood is the concerned in the tributaries, the peak flow time series in tributaries were found to have high variability dominates in the region followed by moderate. Stations at main river also depicted high variability. It can be seen that the CV value of the two river is almost similar in the mean annual and high percentile flow series, which might be a reflection of spatial correlation. CV values are calculated for all stations in high and low flow percentile, and almost all of the stations showed high variability and few of them are moderate. About 83.33% of stations showed high variability in minimum flow (10<sup>th</sup>, 5<sup>th</sup> and 1<sup>st</sup>), and all stations in the 99<sup>th</sup> percentile were found high variability. The two stations (Melka Kunture and Hombole) at the main river course showed moderate variability in high flow (95<sup>th</sup> and 90%). Conversely, main tributaries showed high variability in low flow and high flow. The number of time series exhibited high variability, mainly in tributaries are substantially high. In general, about 50% of the stations in mean annual, 66.6% of the stations in yearly peak flow and 50%

312 of the stations in high and low flow showed above the averaged CV in respective time step, thus flows indices  
 313 experienced high variability.

314 **Table 2** Mean annual, seasonal, peak flow (m<sup>3</sup>/s), and CV of each station at different time scales

Station	Mean		Mean	
	Annual	CV	Peak	CV
Holeta	1.62	0.41	28.29	0.28
Berga	3.21	0.47	51.16	0.47
Teji	3.93	0.52	87.63	0.43
Melka Kunture	29.14	0.28	291.82	0.48
Hombole	43.66	0.27	426.91	0.33
Mojo	11.91	0.77	209.78	0.51
Average		<b>0.45</b>		<b>0.42</b>

315

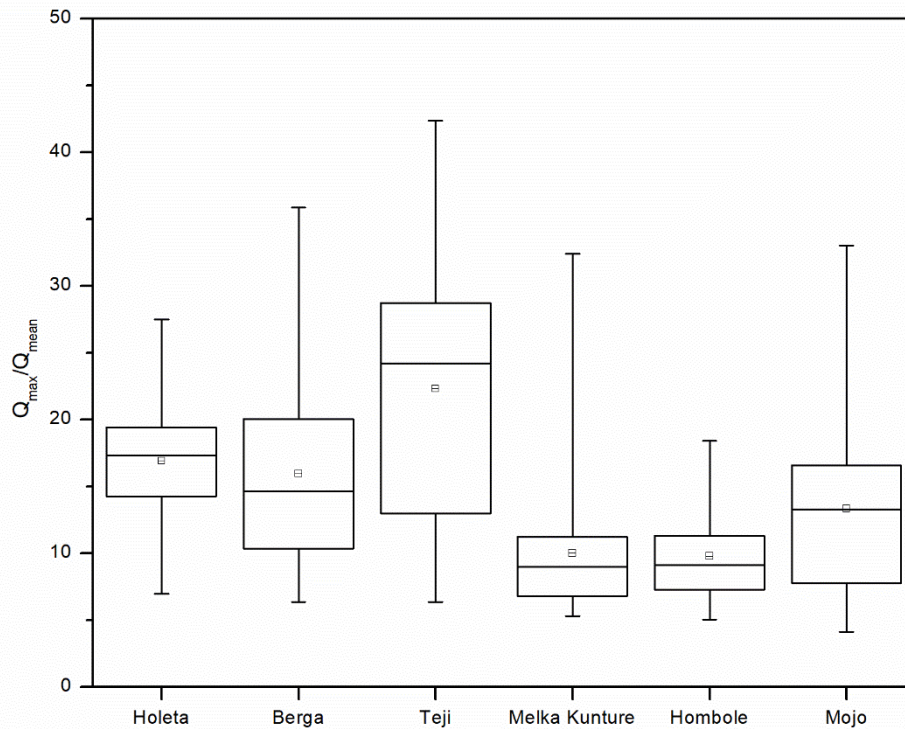
316

317 **Table 3** Mean high and low percentile flows (m<sup>3</sup>/s), and CV of each station at different time scales

Station	Mean		Mean		Mean		Mean		Mean		Mean	
	99th	CV	95th	CV	90th	CV	10th	CV	5th	CV	1st	CV
Holeta	16.10	0.45	7.73	0.77	4.47	0.67	0.18	1.07	0.16	1.20	0.14	1.40
Berga	26.56	0.38	13.78	0.36	9.32	0.41	0.26	1.59	0.23	1.67	0.20	1.82
Teji	43.98	0.53	16.21	0.60	9.76	0.75	0.12	0.93	0.09	0.94	0.08	1.00
Melka Kunture	188.29	0.32	138.32	0.27	111.16	0.29	1.02	0.36	0.77	0.37	0.57	0.38
Hombole	303.38	0.32	206.49	0.29	153.22	0.30	3.34	0.26	2.93	0.27	2.56	0.29
Mojo	114.67	0.66	70.67	0.90	53.49	1.07	0.22	0.53	0.18	0.63	0.14	0.64
Average		<b>0.44</b>		<b>0.53</b>		<b>0.58</b>		<b>0.79</b>		<b>0.85</b>		<b>0.92</b>

318

319 The Flood regime characteristics, the ratio of annual maximum streamflow to mean annual flow  
 320 ( $Q_{max}/Q_{mean}$ ), was calculated for the individual station and shown in Fig. 3, highlighting the division of flood  
 321 magnitude. Thus, one station (Teji) had a significant ratio in the basin. Except at Hombole, the ratio of other  
 322 stations has also resulted in greater than 20. On an average, the ratio was highest at Teji (22.30) upper station  
 323 and lowest at Hombole station (5.0) of the lower station. The highest frequent flood variability was recorded  
 324 recently at Teji station between 2005 and 2014. It was noted that the regression coefficient ( $R^2 = 0.10$ ) exhibited  
 325 a positive relationship, implying area size has an insignificant influence on flood variability. Main tributaries  
 326 stations depicted a higher magnitude of flood regime characteristics, while large flow receiving rivers showed  
 327 lesser (<10).



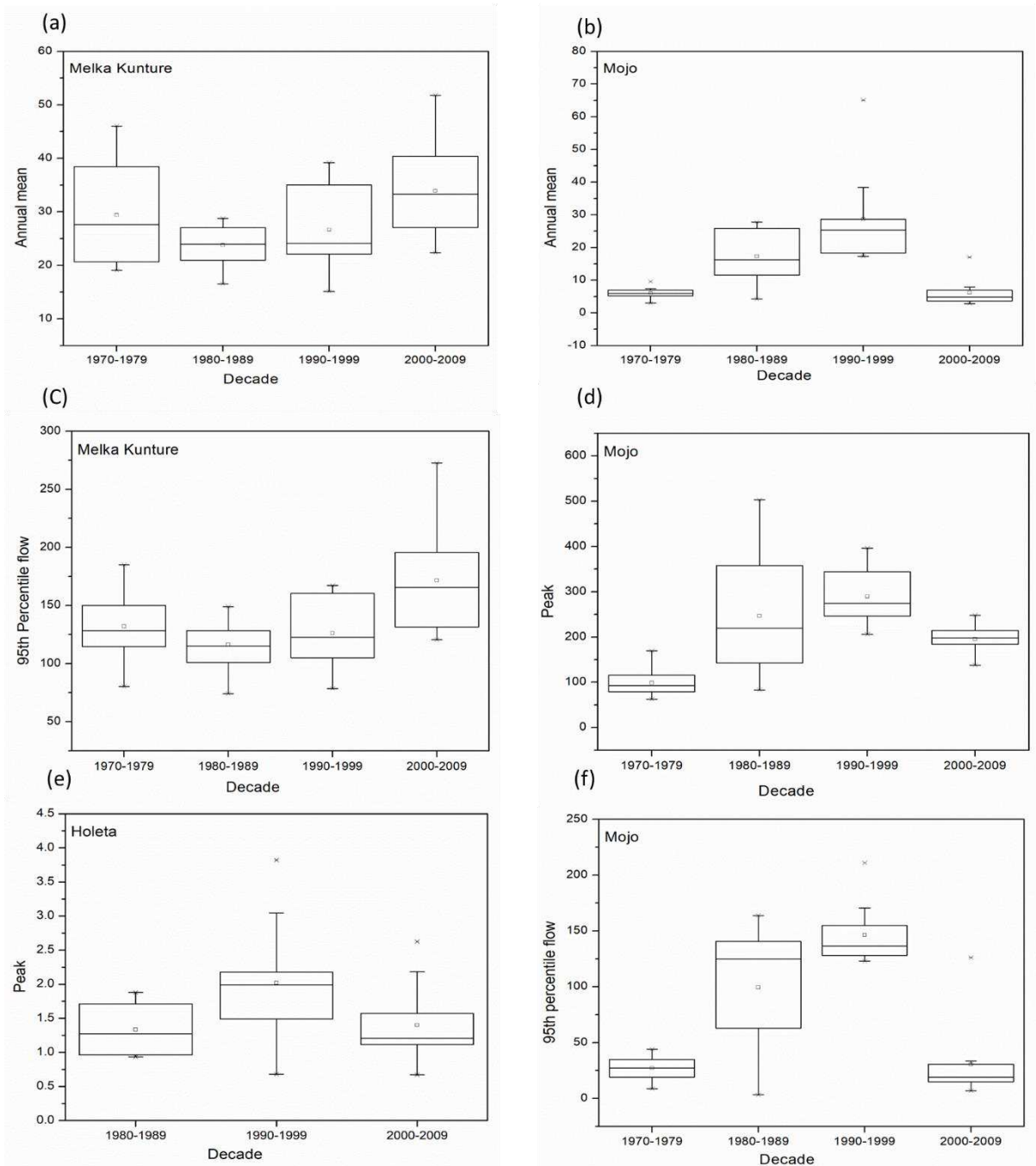
328

329 **Fig. 3** Box-plot of flood variability ranges in terms of maximum, minimum and mean for each station

330 **3.1.2 Inter Decadal Variability**

331 The river discharge changes were evaluated at decadal resolution considering annual mean, peak, 95<sup>th</sup> and 10<sup>th</sup>  
 332 percentile flows series (1970-2009) are representative data sets. Moreover, the data sets were checked against  
 333 variance of the group mean difference is significant. Using Tukey's test, decadal mean flow variability exhibited  
 334 that three stations of the different resolution had a significant difference in mean at  $\alpha = 0.05$ . The mean annual  
 335 discharge of Melka Kunture between the 1980s and 2000s depicted a significant increase and the mean  
 336 difference between the two decades was significantly different (Fig. 4a). The mean variation between the 1970s  
 337 and 1980s, 1970s and 1990s, 1970s and 2000s, 1980s and 1990s, and 1990s and 2000s were insignificant. In  
 338 95<sup>th</sup> percentile flow, the mean significant increase from the 1980s to the 2000s was exhibited (Fig. 4c). In the  
 339 case of Mojo station, the decadal mean annual flow (except for the 1970s and 2000s) variation was significant  
 340 (Fig. 4b). The flow was significantly increased between the 1970s and 1990s and insignificantly decreased from  
 341 the 1990s to 2000s. The 1990s mean annual flow was highly significant compared to the 1970s (Fig. 4b). In  
 342 peak flow, decadal mean variation was a significant increase between the 1970s and 1990s and a significant

343 decrease 1990s and 2000s (Fig. 4d). The highly significant mean difference was shown between the 1970s and  
 344 1990s. The peak flow of the rest decades did not show significant variation. The 95% percentile flow for Mojo  
 345 indicated a significant increase from the 1970s to the 1990s and a significant decrease between the 1990s and  
 346 2000s (Fig. 4f). It is, therefore, apparent mean decadal variations exist between periods.



347

348 **Fig. 4** Decadal variability in different flow indices of various sites of UARB

349 For Holeta peak flow, the mean variations between the 1980s and 2000s was insignificant, but between the  
 350 1980s and 1990s, and 1990s and 2000s, a significant increase and significant decrease was revealed, respectively

351 (Fig. 4e). Thus, significant mean variation presents between the 1980s and 1990s and 1990s and 2000s. Spatially,  
352 Mojo has shown a higher difference in mean peak flow. It can be seen that the 1990s flow has shown an  
353 increasing trend compared to the 1980s and a significant decrease in the 2000s in Mojo and Holeta (except  
354 Melka Kunture).

355 Similar observations were found in Lake Tana basin rivers in Ethiopia (Tigabu et al. 2020). The higher  
356 degree of anomaly flows in these stations are driven by land use, land cover change and climate change. For  
357 instance, Shawul et al. (2019) demonstrated that the urbanization and cropland expansions (1974-1984 and  
358 2000-2014) triggered the variation of surface runoff in Upper Awash river basin (including the Melka Kunture  
359 and Mojo subbasin). In a similar study in the neighbour basin, the expansion of cultivated land and urban areas  
360 has also significantly increased the surface runoff in Andassa watershed, Blue Nile basin (Gashaw et al. 2018).

### 361 **3.1.3 Trend Analysis**

362 A lag one serial correlation coefficient indicates 20 data series of 48 total data series was auto-correlated  
363 significantly in the annual mean, peak flow, and percentiles flow. Thus, considering the serial correlation being  
364 in these time series, a variance correction procedure (Yue and Wang 2004) is crucial before performing trend  
365 analysis to diminish the defects that define the trend in the original MK test. Based on this, the trend results were  
366 discussed in the subsequent sections.

### 367 **3.1.4 Trends in Mean Annual flow**

368 Table 4 presents the summary results of temporal trends by modified MK trend and magnitude of the trends by  
369 Sen's slope in mean annual, peak, high and low percentile flow time step at 5% significance level ( $Z_{critical} =$   
370 1.96). The Z statistics of mean annual was evident that a mixture of positive and negative trends, indicate  
371 increasing and decreasing trends. In most stations, the mean annual series showed that increasing trend but  
372 statistically not significant. MMK statistics exhibited decreasing trend (Holeta and Mojo) and an increasing  
373 trend (Berga, Teji, Melka Kunture and Hombole). The magnitude of decreasing and increasing trend rates using  
374 the Sen's slope were also provided in Table 4. The least trend magnitude was observed in mean annual flow  
375 time series.

376 **Table 4** Value of Z of the Modified Mann-Kendal test (MMK) and Sen's Slope Estimator (SSE) for mean  
377 annual, peak flow, high and low percentile flows

Flow indices	Test	Holeta	Berga	Teji	Melka Kunture	Hombole	Mojo
Mean							
Annual	MMK(Z)	-0.790	1.613	1.199	1.34 <sup>#</sup>	0.606	-0.987 <sup>#</sup>
	SSE	-0.009	0.023	0.023	0.112	0.040	-0.043
Peak	MMK(Z)	-0.160 <sup>#</sup>	2.118 <sup>*</sup>	3.65 <sup>*</sup>	1.592 <sup>#</sup>	-1.881	1.662 <sup>#</sup>
	SSE	-0.016	0.230	1.534	1.795	-1.098	2.086
99th	MMK(Z)	-2.00 <sup>*#</sup>	0.559	2.563 <sup>*</sup>	1.5 <sup>#</sup>	-1.524	-0.456 <sup>#</sup>
	SSE	-0.111	0.039	0.757	0.872	-0.558	-0.234
95th	MMK(Z)	-3.51 <sup>*</sup>	0.669	0.678	1.61 <sup>#</sup>	-0.884	-0.941 <sup>#</sup>
	SSE	-0.093	0.028	0.038	0.554	-0.247	-0.359
90th	MMK(Z)	-5.316 <sup>*</sup>	0.618	-2.243 <sup>*</sup>	1.827	-0.434	-0.566 <sup>#</sup>
	SSE	-0.064	0.016	-0.073	0.604	-0.079	-0.105
10th	MMK(Z)	-5.76 <sup>*</sup>	3.316 <sup>*#</sup>	-5.25 <sup>*#</sup>	0.678	1.626 <sup>#</sup>	2.869 <sup>*</sup>
	SSE	-0.060	0.011	-0.004	0.000	0.011	0.003
5th	MMK(Z)	0.243	3.460 <sup>*#</sup>	-4.758 <sup>*#</sup>	-0.203	1.723 <sup>#</sup>	2.031 <sup>*</sup>
	SSE	0.000	0.009	-0.004	0.000	0.013	0.002
1st	MMK(Z)	-0.585	3.315 <sup>*#</sup>	-5.157 <sup>*#</sup>	1.544	4.312 <sup>*#</sup>	2.446 <sup>*</sup>
	SSE	0.001	0.008	-0.004	0.001	0.021	0.002

378

379

\*and # represent significant trend at 5% significance level, and serially correlated series, respectively.

380

At all stations, MMK statistics result agreed in sign with the result of SSE at 5% significance level. The result indicated that most of the stations in tributaries were characterized by increasing trends and higher trend magnitude in main river section.

381

382

383

The trend of mean annual detected by ITA was presented in Table 5. The result showed that slope S of mean annual flow was dominated by positive values and almost all of them were significant at 95% confidence level. ITA plots illustration of mean annual was shown in Fig. 4. For instance, the ITA for Berga station in mean annual flow, most of the points fall above the 1:1 line indicating increasing trend, further confirms the trend statistics slope S. It has been noted that MMK trend statistics of mean annual flow at Teji and Mojo showed the opposite sign with ITA approach. These signs were also reflected in slope statistics. The spatial patterns of mean annual showed that significant trends were detected almost in all stations. Therefore most of the stations are characterized by significant trends at 5% significance level. Gedefaw et al. (2018) remarked average ITA measured decreasing trends for four annual Awash River discharge stations. However, Hombole and Holeta stations disagreed with the observation for the study period from 1980-2016. These stations have different trends in the time series and direct that the higher point, the stronger the direction.

384

385

386

387

388

389

390

391

392

393

394

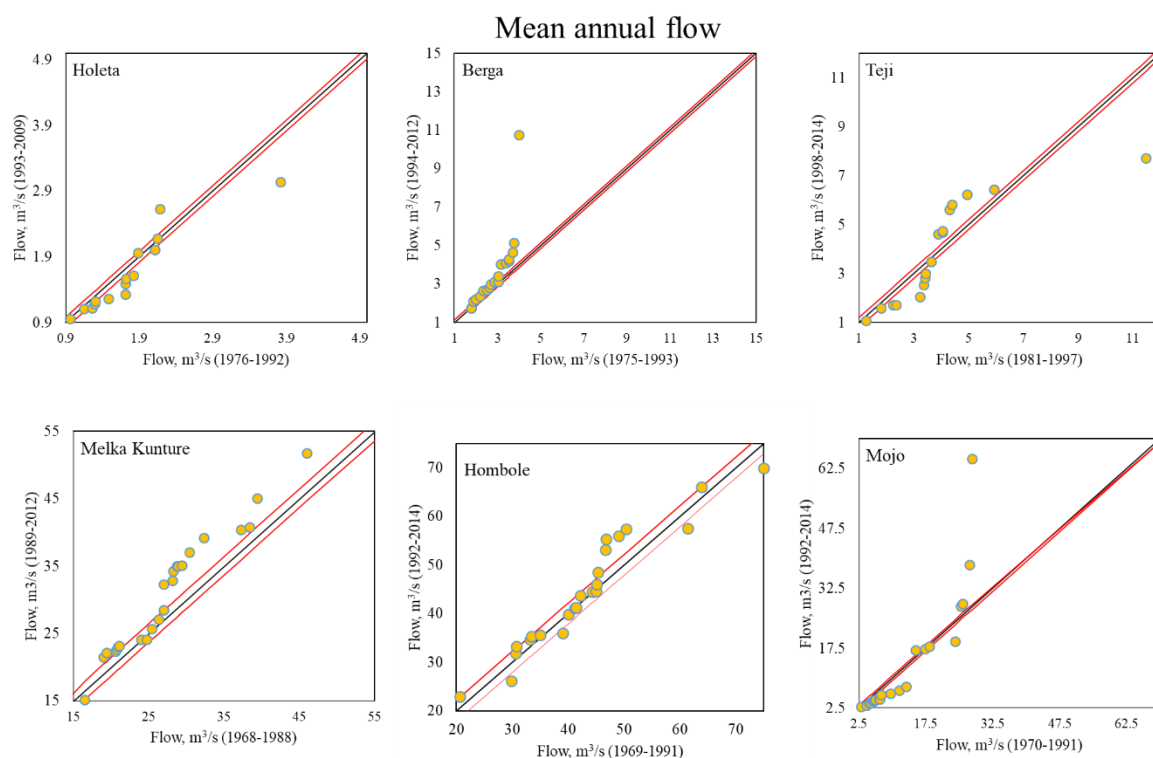
**Table 5** ITA test results of mean annual and Peak flow in six stations

Mean Annual				
Stations	Slope S	Slope Standard Deviation	lower CL at 5% Sign. Level	Upper CL at 5% Sign. Level
Holeta	-0.008*	0.0024	-0.0048	0.0048
Berga	0.041*	0.0085	-0.0166	0.0166
Teji	-0.006	0.0121	-0.0237	0.0237
Melka Kunture	0.134*	0.0117	-0.0229	0.0229
Hombole	0.056*	0.0224	-0.0438	0.0438
Mojo	0.045*	0.0416	-0.0815	0.0815

Peak				
Stations	Slope S	Slope Standard Deviation	lower CL at 5% Sign. Level	Upper CL at 5% Sign. Level
Holeta	-0.044	0.0236	-0.0463	0.0463
Berga	0.327*	0.0435	-0.0852	0.0852
Teji	1.323*	0.0877	-0.1718	0.1718
Melka Kunture	2.748*	0.3516	-0.6892	0.6892
Hombole	-0.891*	0.3118	-0.6111	0.6111
Mojo	1.720*	0.2075	-0.4066	0.4066

395



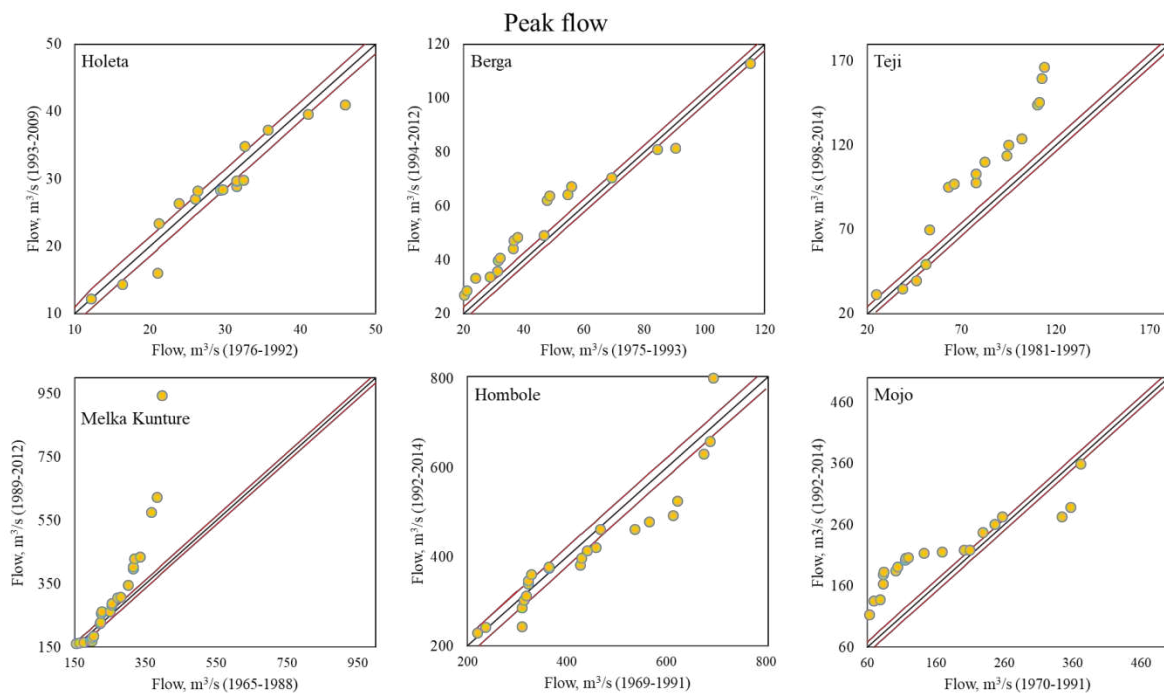
396

397 **Fig. 5** ITA plot results in mean annual flow of each station in UARB

398 **3.1.5 Trends in Peak Flow**

399 The temporal peak flow trends detected by MMK test and trends magnitude by SSE were presented in Table 4.  
 400 In peak flow time series, most of the stations exhibited increasing trends (except Holeta and Hombole); however,  
 401 Significant increasing trends was observed in Teji station ( $1.53 \text{ m}^3/\text{s year}^{-1}$ ) and Berga ( $0.23 \text{ m}^3/\text{s year}^{-1}$ ). The  
 402 decreasing rate of  $1.09 \text{ m}^3/\text{s year}^{-1}$  at 95% confidence level was exhibited at the outlet of Hombole station. The  
 403 spatial pattern of trend magnitude at Mojo station, the increasing rate is as high as  $2.086 \text{ m}^3/\text{s year}^{-1}$ , followed  
 404 by Melka Kunture at rate of  $1.79 \text{ m}^3/\text{s year}^{-1}$ .

405 Peak flow trend test using ITA method was given in Table 5. The result showed that two negative and four  
 406 positive values, but all of them were significant (except at Holeta). The spatial pattern of significant trend from  
 407 upper toward lower river reach, ITA graphical illustration of four increasing stations (Berga, Teji, Melka  
 408 Kunture, and Mojo) and two decreasing stations (Holeta and Hombole) are given in Fig. 5. The ITA plot for  
 409 peak flow shows that most points fall above and below 1:1 line signifying the trend obtained by slope S statistic.  
 410 Peak flow at Berga and Mojo exhibits two different trends in the time series. Then it is possible to see points in  
 411 different regions, for example, lower and upper regions. These indicate non-monotonic trends exist in the time  
 412 series. The upper region (low flow) points are high in number, which shows that the stronger the trend.



413  
 414 **Fig. 6** ITA plot results in peak flow for each station in UARB

415 **3.1.6 Trends in High and Low Percentiles Flows**

416 Stream flow series such as high and low flows are of significant objectives in planning and establishing annual  
417 water balance, in addition to managements of dam’s projects (Diop et al. 2017; Sahoo and Jha 2020). The high  
418 and low flow percentile trends identified by MMK and trend magnitudes by SSE was also summarized in Table  
419 4. Most stations in the high flow categories (99<sup>th</sup>, 95<sup>th</sup> and 90<sup>th</sup>) exhibit decreasing trends, while low flow (10<sup>th</sup>,5<sup>th</sup>  
420 and 1<sup>st</sup>) distribution showed increasing trends at 5% significance level. The high percentile flow of two  
421 tributaries (Teji and Berga) and Melka Kunture identified as increasing but at the out let point showed a  
422 decreasing trends. Of these, Low percentile flow at Berga, Teji and Mojo exhibited a significant trend, but a  
423 very week rate of change per year. Three stations (Berga, Hombole and Mojo) showed a positive significant  
424 trend in low flow. The rate of variation in all stations was revealed much less than unity.

425 The ITA result for high and low flow percentile was presented in Table 6. The slope S of all stations was  
426 obtained and almost all of them were significant at 5% significant level. The high percentile flows were  
427 dominated by negative slope s and significant trends. Spatially, Hombole and Holeta showed significant  
428 downtrend in upper percentile flow. Positive slope S values were found for most of the stations in low percentile  
429 flow and all of them were significant. ITA plots in Fig. further confirm the positive slope S values in these  
430 stations, in which most of the points fall above the 1:1 line. However, composition trends were also observed in  
431 some stations (Teji, Hombole and Mojo) in high flow percentiles.

432  
433  
434  
435  
436  
437  
438  
439  
440  
441  
442

443 **Table 6** ITA test results of percentile flow (90<sup>th</sup>, 95<sup>th</sup>, 90<sup>th</sup> and 10<sup>th</sup>, 5<sup>th</sup> and 1<sup>st</sup>) in six stations

---

99 <sup>th</sup> percentile flow
----------------------------------

---

Stations	Slope		Lower CL at 5% Sign. Level	Upper CL at 5% Sign. Level
	S	Slope Standard Deviation		
Holeta	-0.173*	0.017	-0.033	0.033
Berga	0.192*	0.017	-0.034	0.034
Teji	0.542*	0.050	-0.098	0.098
Melka				
Kunture	1.346*	0.121	-0.237	0.237
Hombole	-0.038*	0.084	-0.164	0.164
Mojo	-0.230*	0.061	-0.120	0.120
95 <sup>th</sup> percentile flow				
Holeta	-0.141*	0.011	-0.021	0.021
Berga	0.100*	0.022	-0.043	0.043
Teji	-0.119	0.063	-0.124	0.124
Melka				
Kunture	0.707*	0.075	-0.146	0.146
Hombole	-0.038	0.084	-0.164	0.164
Mojo	-0.249*	0.099	-0.194	0.194
90 <sup>th</sup> percentile flow				
Holeta	-0.087*	0.015	-0.029	0.029
Berga	0.056*	0.021	-0.041	0.041
Teji	-0.202*	0.063	-0.123	0.123
Melka				
Kunture	0.600*	0.036	-0.070	0.070
Hombole	-0.018	0.088	-0.172	0.172
Mojo	0.171	0.113	-0.221	0.221
10 <sup>th</sup> percentile flow				
Holeta	-0.076*	0.013	-0.025	0.025
Berga	0.017*	0.001	-0.001	0.001
Teji	-0.005*	0.001	-0.001	0.001
Melka				
Kunture	0.005*	0.000	-0.001	0.001
Hombole	0.009*	0.001	-0.002	0.002
Mojo	0.002*	0.001	-0.001	0.001
5 <sup>th</sup> percentile flow				
Holeta	0.005*	0.002	-0.003	0.003
Berga	0.017*	0.001	-0.001	0.001
Teji	-0.005*	0.000	-0.001	0.001
Melka				
Kunture	0.002*	0.001	-0.001	0.001
Hombole	0.010*	0.002	-0.004	0.004
Mojo	0.002*	0.000	-0.001	0.001

444 \* denotes the significant trend at 5% significance level

445

446

447

448 Continued

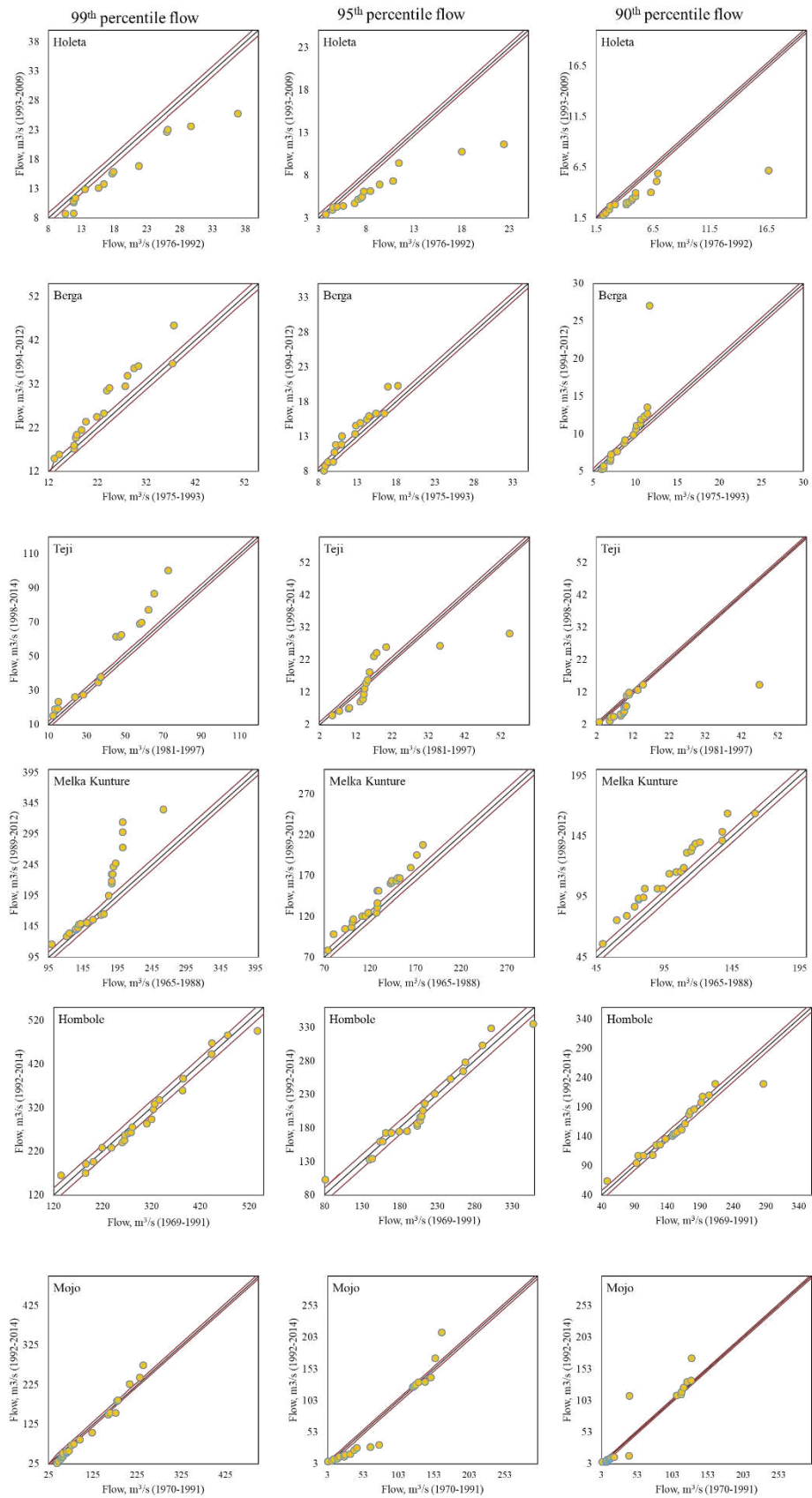
1 <sup>st</sup> percentile flow				
Stations	Slope S	Slope Standard Deviation	Lower CL at 5% Sign. Level	Upper CL at 5% Sign. Level
Holeta	0.004*	0.002	-0.003	0.003
Berga	0.015*	0.001	-0.002	0.002
Teji Melka	0.004*	0.000	-0.001	0.001
Kunture	0.005*	0.000	-0.001	0.001
Hombole	0.017*	0.001	-0.003	0.003
Mojo	0.003*	0.000	0.000	0.000

449

450

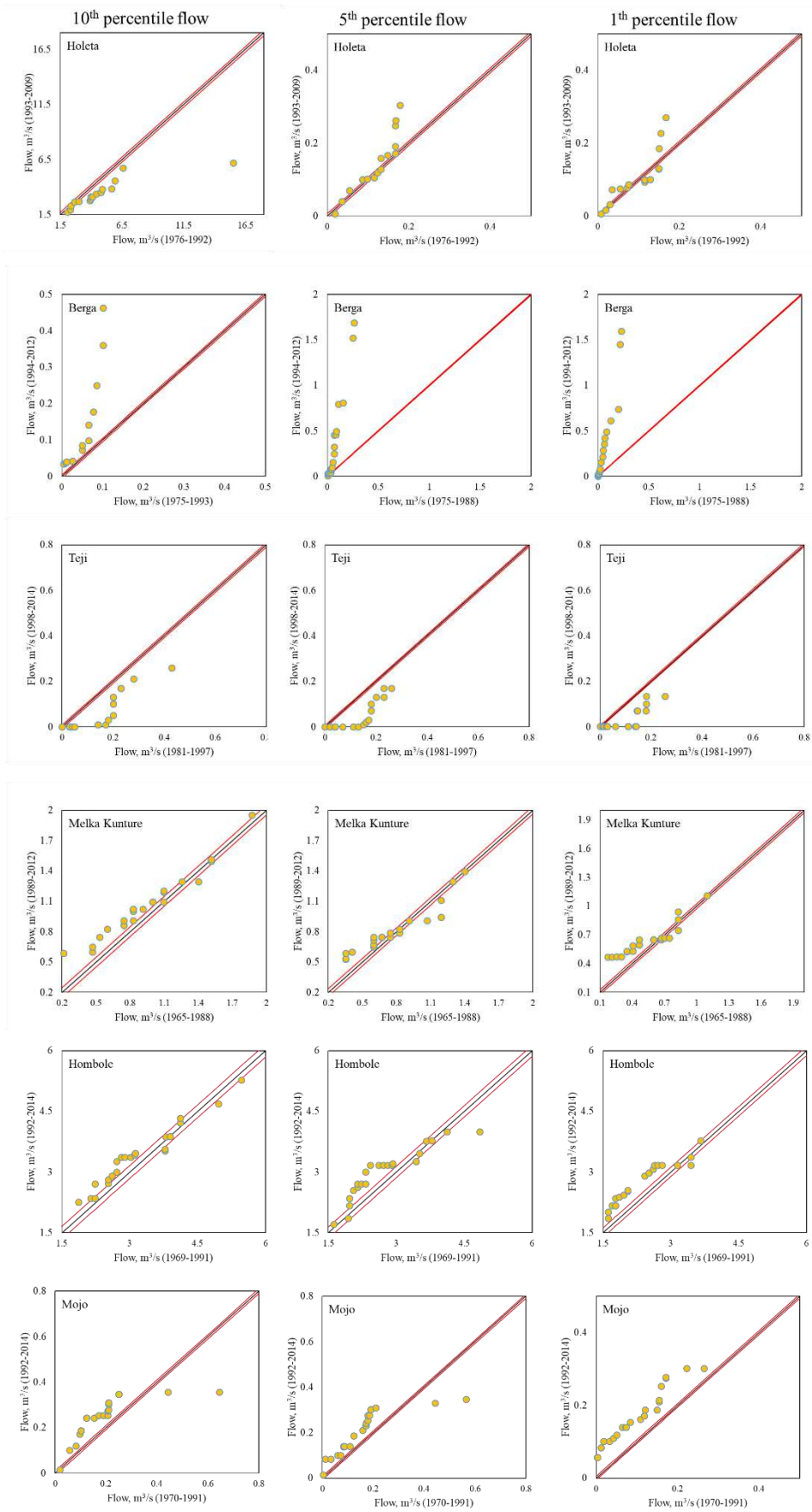
\*Represent significant trend at 5% significance level.

451



452

453 **Fig. 7** ITA plot results of 99th, 95th and 90th flow percentile at each station in UARB



454

455 **Fig. 8** ITA plot results of 10th, 5th and 1st flow percentile at each station in UARB.

456 Generally the amount of flow at the outlet of Hombole site and Mojo station is decreasing and this can  
457 influence the hydropower production from the downstream Koka dam and increase the water stress. The trend  
458 direction of similar stations reported by Tadese et al. (2019) and Daba et al. (2020) showed complete agreement  
459 in annual scale. In the contrary, Gedefaw et al. (2018a) showed seemingly valid results, decreasing for Hombole,  
460 increasing for Holeta, and a significant increase for Berga in annual discharge flow for 1980-2016 at 5 and 10%  
461 significance level using MK and Sen's slope. Thus, the inconsistent result might be due to the start date of data  
462 used for these studies.

463 The decrease of flow across the basin station might be associated with rainfall variability, for instance  
464 Holeta station (Tadese et al. 2019) and Hombole (Daba et al. 2020) and water usage for small irrigation activities  
465 in the basin. Despite the reduction of forest and grass land (increase built up area and cropland) from 1973-2006  
466 in Holeta-Berga watershed (Gelet et al. 2010) and annual rainfall in Addis Alem (Daba et al. 2020)(near to  
467 Berga), the hydrological variables in Berga station showed an increasing trend. In addition another possible  
468 reason to increase the surface runoff was evidenced as land use land cover change in Melka Kunture and Mojo  
469 catchment (Shawul et al. 2019; Zena et al. 2020). Jaweso et al. (2019) indicated that the decrease in rainfall and  
470 increase in temperature consequence negative stream flow trends in the neighboring river basin of Omo Ghibe,  
471 Ethiopia. In other basin, same climatic characteristics, Tekleab et al. (2013) noted varied stream flow trends in  
472 the Abay/Upper Blue Nile basin, Ethiopia and indicated human activities and nature caused the variations. In  
473 addition, Assefa and Moges (2018) found a decreasing trend in low flow in 12 station of the 15 station in Blue  
474 Nile basin, Ethiopia. Land cover change and climate change were claimed responsible resulting in increasing  
475 runoff and evapotranspiration (increasing temperature thereby increasing evaporation from the soil and  
476 decreasing soil water) respectively. Further, Degefu et al. (2019) inspected spatial trends of 10 streamflow  
477 indices using the MK test and Sen's slope estimator at 57 hydrological stations for the highlands of Ethiopia.  
478 They found a significant increase in mean annual, seasonal (dry and wet), maximum and minimum flow  
479 ( $Q_{max/min1day}$ ,  $Q_{max/min7day}$ ,  $Q_{max/min30day}$ ) variables and significant decrease trends in  $Q_{min80p}$  at 5  
480 and 10% significant level. The result is consistent with other basin studies based on the same methodologies.

### 481 **3.1.7 Trend Change-point Analysis**

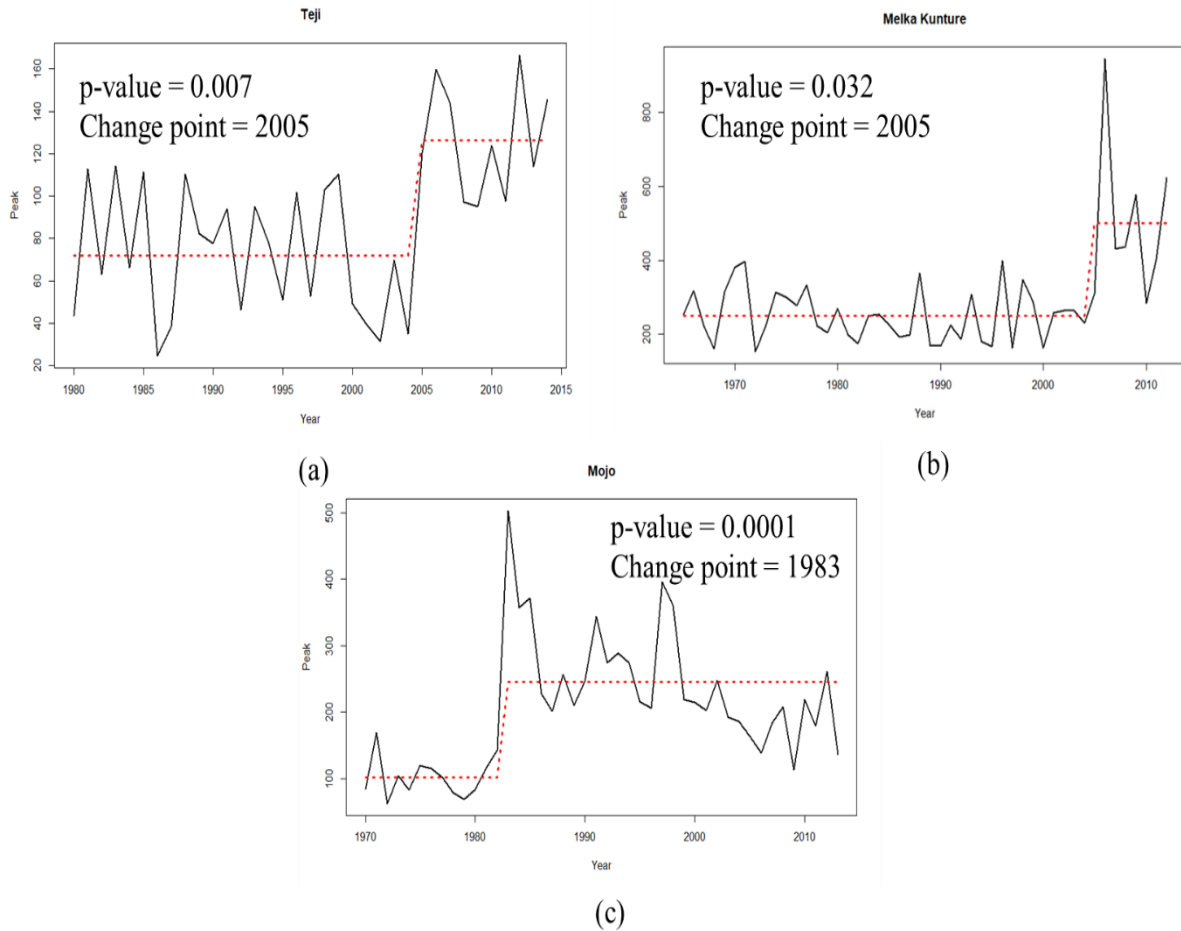
482 Abrupt changes may be attributed to natural or anthropogenic changes in climatic, hydrological or landscape  
483 process (Ryberg et al. 2020). In this study, the Pettitt test was carried out to investigate change point in annual  
484 mean, peak and high and low flow percentile flows considering a 95% confidence level. The change test result

485 was summarized in the Table 7 for stations that showed significant changes in the time series. The change point  
 486 of peak flow for selected stations is displayed in Fig 9. Change points were detected in about 41.6% of the 48  
 487 investigated flow series and upward change was dominant. Most stations have unveiled a significant change  
 488 point in the 2000s, very recently. From the decadal variation analysis in Fig. 4, the change point agrees with the  
 489 mean shift in the 2000s. The significant change point for low percentile flows of Berga station was seen after  
 490 2004. For Teji station, the annual mean, peak and 99<sup>th</sup> percentile flow series breaks upward after 2005. In the  
 491 contrary, in the same station, the significant downward change point in low percentile flows was indicated  
 492 around 1994 and 1995.

493 **Table 7** Table Pettitt test change point summary in a year (p-value < 0.05)

	Station	Berga	Teji	Melka Kunture	Hombole	Mojo
Time series	Annual mean	-	2005	2003	-	2000
	Peak	-	2005	2005	-	1983
	99th	-	2005	2003	-	2000
	95th	-	-	2003	-	2001
	90th	-	-	-	-	2000
	10th	2004	1995	-	-	-
	5th	2004	1994	-	-	-
	1st	2004	1994	-	2005	1990

494  
 495 At the outlet of Hombole station, the low percentile flow (1<sup>st</sup> percentile flow) showed a significant upward  
 496 change in 2005. The second main river Melka Kunture station, exhibited an upward shift in 2003 and 2005 in  
 497 annual mean, high flow percentile and peak flow series, respectively. Mojo station was the highest number of  
 498 break points showed in the time series i.e. in 1983, 1990, 2000 and 2001. This had been reflected in decadal  
 499 variation analysis in Fig. 4 (d). It increased in peak flow and low flow percentile (1<sup>st</sup> percentile flow). Further,  
 500 inter decadal variation analysis confirmed the findings of the change point analysis.



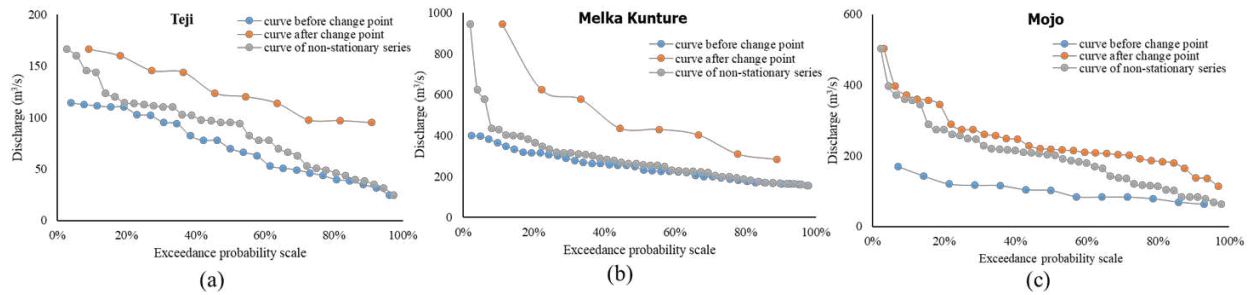
501

502 **Fig. 9** Pettitt test result of peak flow stations a) Teji b) Melka Kunture c) Mojo

503 It is noted that the point change in Teji and Melka Kunture in annual mean, peak flow and high percentile  
 504 flows has occurred at almost the same time, indicating the change in branch station also has an effect on the  
 505 succeeding river station. The two tributaries Teji and Mojo resulted in a significant upward change in peak flow  
 506 at different periods.

507 The hydrological series exhibited trends and change points, which are indicative of the nonstationary  
 508 properties of the hydrological indices. The shape of the probability of exceedence curves before and after a  
 509 breakpoint, and the nonstationary series of the peak flow was shown in Fig. 9. The magnitude of the peak flow  
 510 exceeded or equaled to the specified exceeded probability scales are obtained for comparison before and after  
 511 the change point. In Fig. 9, the exceedence probability curve demonstrated that the peak flow after the change  
 512 point was found upward. For instance, for Teji station, the flood magnitude equaled or exceeded 10%, 50%,  
 513 90% of the time increased by 53.75, 52.14, and 62.66 m<sup>3</sup>/s, respectively. The highest magnitude of change was  
 514 seen in Melka Kunture followed by Mojo after the change point for the specified exceedence probability. Thus,

515 the peak floods after the change point were more significant than the peak flow before the change point equaled  
 516 or exceeded 10%, 50% and 90%.



517  
 518 **Fig. 10** The exceedence probability curve for non-stationary series and series before and after change point: (a)  
 519 Teji (b) Melka Kunture (c) Mojo

520 The results are similar to the estimated trend analysis to flow series in the basin. Zena et al. (2020) reported  
 521 that similar significant change point (in the 2000 year) of the annual mean flow dropped by 80% at Mojo station  
 522 for the period of 1980-2015. During the Bega season (no rain with little flow), the change point was also  
 523 indicated in 1992, which is almost not far from the low flow to our finding (1990) but opposite direction. In  
 524 addition, the authors dictated that climate variability in the watershed has no connection with the decrement of  
 525 surface flow. The comparable changing pattern in a nearby basin, for instance, the mean yearly flow, detected  
 526 an upward shift in two major rivers around the late 1990s, the Upper Omo Ghibe basin of Ethiopia (Jaweso et  
 527 al. 2019). Upward and downwards change points exhibited in different catchments of Abay/Upper Blue Nile  
 528 basin, Ethiopia for 1/7-day annual minimum/maximum flows mostly in 2000s and 1980s (Tekleab et al. 2013).  
 529 The previous study in the Upper Tekeze–Atbara River basin, Ethiopia, Gebremicael et al. (2017) indicated  
 530 decreased low flow (1-day annual minimum flow) after around 2000 and high flow (1-day maximum yearly)  
 531 increased after 1995. In sum, this significant increment in peak flow in the tributaries, mainly upstream,  
 532 exacerbates the continuing flooding during the heavy rain periods (July and August). Thus, the increasing human  
 533 activities impact flooding and water availability in the future should be the primary concern, principally seasonal  
 534 peak flow and requisite land-use management intervention in the basin.

### 535 3.1.8 Comparison of modified MK trend test and ITA

536 For the 12 mean annual and peak flow series evaluated by the MMK test and ITA method at 5% significant  
 537 level, significant trends were observed in 2 series by MMK test and 8 series by ITA method. ITA also detected

538 all significant trends identified by MMK test. The two trend analysis approaches revealed that 2 series in annual  
539 mean were inconsistent with the sign of the trend (opposite each other). It was also noted such difference by two  
540 methods in hydroclimatic trend assessment (Belihu et al. 2018). It is noted that there was complete agreement  
541 in directions between the trend tests, 8 increasing and 4 decreasing trends (including significant) by ITA and 8  
542 increasing trends (including significant) and 4 decreasing trends by MMK test method. Also, the ITA method  
543 detected significant trends in mean annual and peak flow series that the MMK test has not identified. The trends  
544 statistics in the 36 high and low flow percentile series by MMK and ITA show that significant trends/directions  
545 were detected in 16 series by MMK and 32 series by ITA method, including the significant trends identified by  
546 MMK test. The 4 series in the high and low flow percentile showed disagreement with the trend sign. In sum,  
547 the closing agreement is observed between the MMK and ITA, 20 increasing and 16 decreasing trends were  
548 identified by MMK and 23 increasing and 13 decreasing trends were also seen by ITA including significant  
549 trend. In these tests, significant trends in time series that are not recognized by the MMK test are successfully  
550 spotted by ITA tests. ITA approached revealed more significant trends in the time series (increasing and  
551 decreasing trends) and included all significant trends identified by MMK.

552 In the present study, the agreement among the signs of the trends is observed but is not entirely consistent  
553 with significant trends. ITA method proved the ability to graphically show the non-monotonic trends in the same  
554 time series or hidden trends compared to the MMK test, helping to examine the flow properties in groups. It is  
555 rational to use ITA method to scrutinize the sub-trend in hydrological series rationally. In the case of this study,  
556 it was seen that the high flow region shows a substantial increase and decrease. As far as the flood is concerned  
557 in the region, the significant increase of high group in peak flow of the Melka Kunture station was observed.  
558 The present study performed a very different look from classical trend analysis for high-resolution hydrological  
559 data series. The classical MK and Sen's slope give overall trends directions and do not provide sub-trends  
560 graphically and respective quantitative estimation. Thus, ITA delivers clear insight into the temporal variability  
561 of hydrological series and is crucial to identifying the flow cluster that is increasing or decreasing for effective  
562 management of extreme hydrologic events in the basin.

563 In summary, it is essential to note that discharge variability varies spatially in terms of mean annual, peak,  
564 and percentiles flow under the investigated stations. Almost all of the stations in tributaries (upper, middle and  
565 lower reach) of UARB showed moderate to high variability (CV) in mean annual and peak flow, respectively.  
566 High variability was detected in tributaries (upper, middle and lower reach) in high and low percentile flow. The

567 main rivers (Melka Kunture and Hombole) showed moderate to high variability in most stations and were  
568 dominated by moderate variability. The result demonstrated a very close coefficient of variation values to mean  
569 annual, as Tadese et al. (2019) stated. The above discussions were consistent with (Billi et al. 2014) reported  
570 that the annual runoff shows a broader range of variation among rivers in Ethiopia. Dettinger and Diaz (2000)  
571 note the average year-to-year CV of streamflow across the globe is 0.49. The flood variability behaviour in  
572 tributaries was found to be higher than in the main river. The high variability in low flow percentiles in tributaries  
573 results in water deficiency for agricultural irrigation activities over the UARB. The decadal variation of  
574 hydrological series exhibited a significant difference in mean in mean annual, peak and 95<sup>th</sup> percentile flow and  
575 was found to be related with detected change points.

576 In the past years, in different regions of the world, a non-parametric approach was used to evaluate the  
577 hydrological series (Arrieta-Castro et al. 2020; Sahoo and Jha 2020). Spatial hydrological variability studies at  
578 various scales have been indicated as very important for effective water resources management and planning for  
579 present and future demands (Kuriqi et al. 2020) in the basin. In this study, the trend of eight flow indices were  
580 evaluated by using the modified MK test (variance corrected based) and ITA at 5% significant level. It was  
581 noted that there was complete agreement in directions between the trend tests, and ITA detected all significant  
582 trends identified by MMK test. Spatially, increasing trends in mean annual and peak flow were dominant in  
583 tributaries. The decreasing trends were noticed in high percentile flow at Homoble outlet and its adjacent Mojo  
584 River, but oppositely the low percentile flows were increased. The low percentile flow in the tributaries was  
585 shown a significant increase in Berga and a decrease (no trend magnitude) in Teji and Holeta. The Pettitt test  
586 detected a significant change point in the 2000s, mostly an upward direction and the peak flow point out that  
587 most stations in tributaries, including the main river Melka Kunture detected an upward change.

588 In support of the present study, several studies have analysed trends in flow indices in other parts of the  
589 world and point out the possible drivers. The possible shift or trend change in record data over time is mostly  
590 associated with the remarkably changing environment, global and local climate variability and land-use  
591 dynamics (Wagesho et al. 2012) and nature (Arrieta-Castro et al. 2020). Sahoo and Jha (2020) indicated low  
592 flow affected by the land cover change and water storage structures. In the present context, UARB, the potential  
593 cause for streamflow change in the majority of subbasin might be linked to rainfall distribution and land cover  
594 change. Other possible factors, such as antecedent soil moisture (Wasko and Nathan 2019) in the basin can be  
595 attributed to an increase or decrease in discharge flows.

596 The study of streamflow characteristics in planning and developmental activities such as hydropower,  
597 irrigation, water supply projects, drought and flood, its impacts on operational and efficient functioning are  
598 imperative. In hydroclimatological time series observation, the recent human activities and climate variation are  
599 two major determinant factors that invalidate the stationary assumption in hydrological studies (Milly et al.  
600 2008). Thus, hydrological studies, water resource planning and management to account the adjusting land cover  
601 land use and climate change in the basin. Therefore, in agreement with this study, it was seen that the UARB  
602 streamflow trend and change matches with previous studies in and around the region. This study examined the  
603 spatial characteristics of temporal trends and change in peak, high and low flow percentiles time series in high  
604 resolution. The spatiotemporal depth analysis of river discharge provides insight into better water resources and  
605 flood management in the basin. Thus, the detail information of flow characteristics can be described using higher  
606 resolution than the courser (e.g. seasonal flow evaluation).

#### 607 **4 Conclusions**

608 The study aimed to investigate hydrological variability, trend and change in hydrological indices of the UARB.  
609 Statistical tests such as coefficient of variation were used to explore the variability, flood variability to  
610 characterize the flood regime and Tukey's test to evaluate decadal mean variation. The modified MK test, SSE  
611 and recent ITA were also applied to detect trends and Pettitt's test to identify probable change time in  
612 hydrological time series in different time steps, annual mean, annual peak, and upper and lower percentile scale  
613 at 5% significance level. Based on the assessment attempted, the spatial flow indices variability, trend and  
614 change over the basin were concluded as follow:

615 Rivers discharge varies spatially from the lower amount in the upper to higher in the lower reach. The  
616 interannual coefficient of variation of UARB was portrayed as moderate to high variability in discharge series  
617 and most of them exhibited high variability. Flood regime characteristics were found higher in main tributaries  
618 than the main river, implying high discharge variability in branches. The spatial pattern of the variability in  
619 tributaries was exhibited as high. Tukey's multiple mean difference comparison technique was applied and few  
620 stations series showed significant differences between the mean of groups. Significance increase and decrease  
621 in mean difference between the mean of groups was noted and enabled to confirm the change point, for instance,  
622 in the 2000s.

623 The serial correlation test identified most of the station time series were serially correlated. Based on the  
624 assessment, a modified Mk test based on the variance correction techniques was utilized to reduce the effect of  
625 autocorrelation. The modified MK test and ITA, and SSE revealed increasing trends were dominant, followed  
626 by decreasing trends in the basin at 5% significant level in the all-time series considered in the study. Significant  
627 decreases and increases were identified in low percentile flow in tributaries. The higher magnitude of increase  
628 was revealed in the branch river in peak flow series at Mojo station. Notably, it was noted that there was an  
629 agreement between the two trend analysis approaches in terms of positive and negative statistics values. In some  
630 series, the opposite sign of trends was identified. The two trend analysis methods were able to signify the  
631 temporal hydrological variability over the basin, but the ITA method can detect the sub-trends than the modified  
632 MK test and does not require a serial correlation test in time series. Based on these assessments, the discharge  
633 variability in all-time steps in tributaries was dominated by positive trends, including Melka Kunture (the main  
634 river). Overall at the outlet point of Hombole site, flow indices experienced a negative trend in peak and high  
635 percentile flow compared to the annual mean and low percentile flow, which shows a positive trend.

636 Using Pettitt's test, change point analysis revealed that the annual mean, peak flow, and high percentile flow  
637 commonly exhibited significant probable shift points in the 2000s and low percentile flow in the 1990s. Most  
638 station's time series showed a significant upward shift (except Teji low percentile flow). Climate variability,  
639 land cover change, water withdrawal for agricultural irrigation are possible mechanisms responsible for changes  
640 in streamflow indices.

641 Higher resolutions of diverse data scales are essential to remark the difference in the spatiotemporal  
642 variability of river discharge and able to detect in depth variation. The flow variability reflects the causes and  
643 probability of flood and drought in the tributaries. Integrated water resources management is necessitated to  
644 overcome the water resources management aspects and flow control severely limits variability in the tributary.  
645 The study provides an understanding of water resources variability in depth, which will be necessary to apply  
646 operational water resources strategies and management to restrain the potential impacts.

647

648

## 649 **Acknowledgments**

650 The authors acknowledge the Ethiopian ministry of water resources, irrigation and electricity for providing  
651 hydrological data.

652 **Funding**

653 Not applicable.

654 **Authors' contributions**

655 Sintayehu Yadete Tola: conceptualized, methodology, analyze study data, results and discussion and  
656 conclusions. Amba Shetty: supervised the study and edited the manuscript. All authors read and approved the  
657 manuscript.

658 **Availability of data and material**

659 All data generated or analysed during this study are included in this article.

660 **Code Availability**

661 Not applicable.

662 **Declarations**

663 **Ethical approval**

664 Not applicable.

665 **Consent to Participate**

666 Not applicable.

667 **Consent for publication**

668 Not applicable.

669 **Conflict interest**

670 The authors declare that they have no competing interests.

671 **Authors' information**

672 <sup>1</sup>Department of Water Supply and Environmental Engineering, Arba Minch Water Technology Institute, Arba  
673 Minch University PO. Box 21, Ethiopia. Ph.D. Research Scholar, Department Water Resources and Ocean  
674 Engineering, National Institute of Technology Karnataka, Srinivasnagar Surathkal, Mangalore, Karnataka,  
675 575025, India.

676 <sup>2</sup>Department of Water Resources and Ocean Engineering, National Institute of Technology Karnataka,  
677 Srinivasnagar Surathkal, Mangalore, Karnataka, 575025, India.

679 **References**

- 680 Ali R, Kuriqi A, Abubaker S, Kisi O (2019) Long-term trends and seasonality detection of the observed flow in  
681 Yangtze River using Mann-Kendall and Sen's innovative trend method. *Water (Switzerland)* 11:.  
682 <https://doi.org/10.3390/w11091855>
- 683 Apollonio C, Balacco G, Novelli A, et al (2016) Land use change impact on flooding areas: The case study of  
684 Cervaro Basin (Italy). *Sustain* 8:. <https://doi.org/10.3390/su8100996>
- 685 Arrieta-Castro M, Donado-Rodríguez A, Acuña GJ, et al (2020) Analysis of streamflow variability and trends in  
686 the meta river, Colombia. *Water (Switzerland)* 12:.. <https://doi.org/10.3390/w12051451>
- 687 Asadieh B, Krakauer NY (2017) Global change in streamflow extremes under climate change over the 21st  
688 century. *Hydrol Earth Syst Sci* 21:5863–5874. <https://doi.org/10.5194/hess-21-5863-2017>
- 689 Assefa K, Moges MA (2018) Low Flow Trends and Frequency Analysis in the Blue Nile Basin, Ethiopia. *J*  
690 *Water Resour Prot* 10:182–203. <https://doi.org/10.4236/jwarp.2018.102011>
- 691 Ay M, Kisi O (2015) Investigation of trend analysis of monthly total precipitation by an innovative method.  
692 *Theor Appl Climatol* 120:617–629. <https://doi.org/10.1007/s00704-014-1198-8>
- 693 Azam M, Maeng SJ, Kim HS, et al (2018) Spatial and temporal trend analysis of precipitation and drought in  
694 South Korea. *Water (Switzerland)* 10:.. <https://doi.org/10.3390/w10060765>
- 695 Bao Z, Zhang J, Wang G, et al (2019) The impact of climate variability and land use/cover change on the water  
696 balance in the Middle Yellow River Basin, China. *J Hydrol* 577:123942.  
697 <https://doi.org/10.1016/j.jhydrol.2019.123942>
- 698 Bard A, Renard B, Lang M, et al (2015) Trends in the hydrologic regime of Alpine rivers. *J Hydrol* 529:1823–  
699 1837. <https://doi.org/10.1016/j.jhydrol.2015.07.052>
- 700 Bekele D, Alamirew T, Kebede A, et al (2017) Analysis of rainfall trend and variability for agricultural water  
701 management in awash river Basin, Ethiopia. *J Water Clim Chang* 8:127–141.  
702 <https://doi.org/10.2166/wcc.2016.044>
- 703 Belayneh A, Adamowski J, Khalil B, Ozga-Zielinski B (2014) Long-term SPI drought forecasting in the Awash  
704 River Basin in Ethiopia using wavelet neural networks and wavelet support vector regression models. *J*  
705 *Hydrol* 508:418–429. <https://doi.org/10.1016/j.jhydrol.2013.10.052>
- 706 Belihu M, Abate B, Tekleab S, Bewket W (2018) Hydro-meteorological trends in the Gidabo catchment of the  
707 Rift Valley Lakes Basin of Ethiopia. *Phys Chem Earth, Parts A/B/C* 104:84–101.  
708 <https://doi.org/10.1016/j.pce.2017.10.002>
- 709 Billi P, Alemu YT, Ciampalini R (2013) The increased frequency of flash floods in Ethiopia: climate change or  
710 human impact? *Nat Hazards* 76:1373–1394
- 711 Billi P, Fazzini M, Alemu YT, Ciampalini R (2014) Rainfall and runoff variability in Ethiopia. 16:7397
- 712 Blöschl G, Ardoin-Bardin S, Bonell M, et al (2007) At what scales do climate variability and land cover change  
713 impact on flooding and low flows? *Hydrol Process* 21:1241–1247. <https://doi.org/10.1002/hyp.6669>
- 714 Caloiero T, Coscarelli R, Ferrari E (2018) Application of the Innovative Trend Analysis Method for the Trend  
715 Analysis of Rainfall Anomalies in Southern Italy. *Water Resour Manag* 32:4971–4983.  
716 <https://doi.org/10.1007/s11269-018-2117-z>
- 717 Chen J, Wu X, Finlayson BL, et al (2014) Variability and trend in the hydrology of the Yangtze River, China:  
718 Annual precipitation and runoff. *J Hydrol* 513:403–412. <https://doi.org/10.1016/j.jhydrol.2014.03.044>
- 719 Daba MH, Ayele GT, You S (2020) Long-Term Homogeneity and Trends of Hydroclimatic Variables in Upper  
720 Awash River Basin, Ethiopia. *Adv Meteorol* 2020:1–21. <https://doi.org/10.1155/2020/8861959>
- 721 Daba MH, You S (2020) Assessment of climate change impacts on river flow regimes in the upstream of awash  
722 basin, ethiopia: Based on ipcc fifth assessment report (ar5) climate change scenarios. *Hydrology* 7:1–22.  
723 <https://doi.org/10.3390/hydrology7040098>

- 724 Degefu MA, Alamirew T, Zeleke G, Bewket W (2019) Detection of trends in hydrological extremes for  
725 Ethiopian watersheds, 1975–2010. *Reg Environ Chang* 19:1923–1933. [https://doi.org/10.1007/s10113-](https://doi.org/10.1007/s10113-019-01510-x)  
726 019-01510-x
- 727 Dettinger MD, Diaz HF (2000) Global characteristics of stream flow seasonality and variability. *J*  
728 *Hydrometeorol* 1:289–310. [https://doi.org/10.1175/1525-7541\(2000\)001<0289:GCOSFS>2.0.CO;2](https://doi.org/10.1175/1525-7541(2000)001<0289:GCOSFS>2.0.CO;2)
- 729 Diop L, Yaseen ZM, Bodian A, et al (2017) Trend analysis of streamflow with different time scales: a case  
730 study of the upper Senegal River. *ISH J Hydraul Eng* 24:105–114.  
731 <https://doi.org/10.1080/09715010.2017.1333045>
- 732 Drissia TK, Jothiprakash V, Anitha AB (2019) Statistical classification of streamflow based on flow variability  
733 in west flowing rivers of Kerala, India. *Theor Appl Climatol* 137:1643–1658.  
734 <https://doi.org/10.1007/s00704-018-2677-0>
- 735 Edossa DC, Babel MS, Gupta A Das (2010) Drought analysis in the Awash River Basin, Ethiopia. *Water*  
736 *Resour Manag* 24:1441–1460. <https://doi.org/10.1007/s11269-009-9508-0>
- 737 Gashaw T, Tulu T, Argaw M, Worqlul AW (2018) Modeling the hydrological impacts of land use/land cover  
738 changes in the Andassa watershed, Blue Nile Basin, Ethiopia. *Sci Total Environ* 619–620:1394–1408.  
739 <https://doi.org/10.1016/j.scitotenv.2017.11.191>
- 740 Gebremicael TG, Mohamed YA, Zaag P, Hagos EY (2017) Temporal and spatial changes of rainfall and  
741 streamflow in the Upper Tekez e – Atbara river basin , Ethiopia. 2127–2142.  
742 <https://doi.org/10.5194/hess-21-2127-2017>
- 743 Gedefaw M, Wang H, Yan D, et al (2018) Trend analysis of climatic and hydrological variables in the Awash  
744 river basin, Ethiopia. *Water (Switzerland)* 10:1–14. <https://doi.org/10.3390/w10111554>
- 745 Gelet M, Suryabhadgavan K V., Balakrishnan M (2010) Land-use and Landscape Pattern Changes in Holeta-  
746 Berga Watershed, Ethiopia. *Int J Ecol Environ Sci* 36:
- 747 Gudmundsson L, Do HX, Leonard M, Westra S (2018) The Global Streamflow Indices and Metadata Archive  
748 (GSIM)-Part 2: Quality control, time-series indices and homogeneity assessment. *Earth Syst Sci Data*  
749 10:787–804. <https://doi.org/10.5194/essd-10-787-2018>
- 750 Guo H, Hu Q, Jiang T (2008) Annual and seasonal streamflow responses to climate and land-cover changes in  
751 the Poyang Lake basin, China. *J Hydrol* 355:106–122. <https://doi.org/10.1016/j.jhydrol.2008.03.020>
- 752 Hailemariam K (1999) Impact of climate change on the water resources of Awash River Basin, Ethiopia. *Clim*  
753 *Res* 12:91–96. <https://doi.org/10.3354/cr012091>
- 754 Hansford MR, Plink-Björklund P, Jones ER (2020) Global quantitative analyses of river discharge variability  
755 and hydrograph shape with respect to climate types. *Earth-Science Rev* 200:102977.  
756 <https://doi.org/10.1016/j.earscirev.2019.102977>
- 757 IPCC (2014) *Climate Change : Impacts, Adaptation, and Vulnerability. Part B: Regional Aspects. Contribution*  
758 *of Change., Working Group II to the Fifth Assessment Report of the Intergovernmental Panel on Climate*
- 759 Jaiswal RK, Lohani AK, Tiwari HL (2015) Statistical Analysis for Change Detection and Trend Assessment in  
760 Climatological Parameters. *Environ Process* 2:729–749. <https://doi.org/10.1007/s40710-015-0105-3>
- 761 Jaweso D, Abate B, Bauwe A, Lennartz B (2019) Hydro-meteorological trends in the upper Omo-Ghibe river  
762 basin, Ethiopia. *Water (Switzerland)* 11:1–18. <https://doi.org/10.3390/w11091951>
- 763 Jha M, Pan Z, Tackle ES, Gu R (2004) Impacts of climate change on streamflow in the Upper Mississippi River  
764 Basin: A regional climate model perspective. *J Geophys Res D Atmos* 109:1–12.  
765 <https://doi.org/10.1029/2003JD003686>
- 766 Kendall M (1975) *Rank correlation methods*. Charles Griffin, London
- 767 Kisaka MO, Mucheru-Muna M, Ngetich FK, et al (2015) Rainfall Variability, Drought Characterization, and  
768 Efficacy of Rainfall Data Reconstruction: Case of Eastern Kenya. *Adv Meteorol* 2015:1–16.  
769 <https://doi.org/10.1155/2015/380404>
- 770 Kisi O (2015) An innovative method for trend analysis of monthly pan evaporations. *J Hydrol* 527:1123–1129.

- 771 <https://doi.org/10.1016/j.jhydrol.2015.06.009>
- 772 Kundzewicz ZW, Robson AJ (2004) Change detection in hydrological records - A review of the methodology.  
773 *Hydrol Sci J* 49:7–19. <https://doi.org/10.1623/hysj.49.1.7.53993>
- 774 Kuriqi A, Ali R, Pham QB, et al (2020) Seasonality shift and streamflow flow variability trends in central India.  
775 *Acta Geophys* 68:1461–1475. <https://doi.org/10.1007/s11600-020-00475-4>
- 776 Legesse D, Abiye TA, Vallet-Coulomb C, Abate H (2010) Streamflow sensitivity to climate and land cover  
777 changes: Meki River, Ethiopia. *Hydrol Earth Syst Sci* 14:2277–2287. <https://doi.org/10.5194/hess-14-2277-2010>
- 778
- 779 Legesse D, Vallet-Coulomb C, Gasse F (2003) Hydrological response of a catchment to climate and land use  
780 changes in Tropical Africa: Case study south central Ethiopia. *J Hydrol* 275:67–85.  
781 [https://doi.org/10.1016/S0022-1694\(03\)00019-2](https://doi.org/10.1016/S0022-1694(03)00019-2)
- 782 Liu Z, Cuo L, Li Q, et al (2020) Impacts of climate change and land use/cover change on streamflow in  
783 beichuan river basin in Qinghai Province, China. *Water (Switzerland)* 12:.  
784 <https://doi.org/10.3390/W12041198>
- 785 Ljung G, Box G (1978) On a measure of lack of fit in time series models. *Biometrika* 65:297–303
- 786 Mann HB (1945a) Nonparametric Tests Against Trend. *Econometrica* 13:245. <https://doi.org/10.2307/1907187>
- 787 Mann HB (1945b) Nonparametric Tests Against Trend. *Econometrica* 13:245. <https://doi.org/10.2307/1907187>
- 788 Meresa HK, Romanowicz RJ, Napiorkowski JJ (2017) Understanding changes and trends in projected  
789 hydroclimatic indices in selected Norwegian and Polish catchments. *Acta Geophys* 65:829–848.  
790 <https://doi.org/10.1007/s11600-017-0062-5>
- 791 Milly PCD, Betancourt J, Falkenmark M, et al (2008) Climate change: Stationarity is dead: Whither water  
792 management? *Science (80- )* 319:573–574. <https://doi.org/10.1126/science.1151915>
- 793 Mulugeta S, Fedler C, Ayana M (2019) Analysis of long-term trends of annual and seasonal rainfall in the  
794 Awash River Basin, Ethiopia. *Water (Switzerland)* 11:.  
<https://doi.org/10.3390/w11071498>
- 795 Nie W, Yuan Y, Kepner W, et al (2011) Assessing impacts of Landuse and Landcover changes on hydrology for  
796 the upper San Pedro watershed. *J Hydrol* 407:105–114. <https://doi.org/10.1016/j.jhydrol.2011.07.012>
- 797 Nilawar AP, Waikar ML (2019) Impacts of climate change on streamflow and sediment concentration under  
798 RCP 4.5 and 8.5: A case study in Purna river basin, India. *Sci Total Environ* 650:2685–2696.  
799 <https://doi.org/10.1016/j.scitotenv.2018.09.334>
- 800 Orke YA, Li M (2021) Hydroclimatic Variability in the Bilate Watershed, Ethiopia
- 801 Palmer MA, Reidy Liermann CA, Nilsson C, et al (2008) Climate change and the world’s river basins:  
802 Anticipating management options. *Front Ecol Environ* 6:81–89. <https://doi.org/10.1890/060148>
- 803 Partal T, Kahya E (2006) Trend analysis in Turkish precipitation data. *Hydrol Process* 20:2011–2026.  
804 <https://doi.org/10.1002/hyp.5993>
- 805 Petrow T, Merz B (2009) Trends in flood magnitude, frequency and seasonality in Germany in the period 1951-  
806 2002. *J Hydrol* 371:129–141. <https://doi.org/10.1016/j.jhydrol.2009.03.024>
- 807 Pettitt AN (1979) A Non-Parametric Approach to the Change-Point Problem. *Appl Stat* 28:126.  
808 <https://doi.org/10.2307/2346729>
- 809 Rao, Hamed (2000) *Flood Frequency Analysis*. CRC Press LLC
- 810 Ruwangika AM, Perera A, Rathnayake U (2020) Comparison of Statistical , Graphical , and Wavelet Transform  
811 Analyses for Rainfall Trends and Patterns in Badulu Oya Catchment , Sri Lanka. 2020:
- 812 Ryberg KR, Hodgkins GA, Dudley RW (2020) Change points in annual peak streamflows: Method comparisons  
813 and historical change points in the United States. *J Hydrol* 583:124307.  
814 <https://doi.org/10.1016/j.jhydrol.2019.124307>
- 815 Sahoo BB, Jha R (2020) Assessment of low flow trends and change point detection in Mahanadi River basin,

- 816 India. *Sustain Water Resour Manag* 6:1–14. <https://doi.org/10.1007/s40899-020-00441-4>
- 817 Sen P (1968) Estimates of the regression coefficient based on Kendall's tau. *J Am Stat Assoc* 63:1379–1389
- 818 Şen Z (2017) Innovative trend significance test and applications. *Theor Appl Climatol* 127:939–947.  
819 <https://doi.org/10.1007/s00704-015-1681-x>
- 820 Şen Z (2012) Innovative Trend Analysis Methodology. *J Hydrol Eng* 17:1042–1046.  
821 [https://doi.org/10.1061/\(asce\)he.1943-5584.0000556](https://doi.org/10.1061/(asce)he.1943-5584.0000556)
- 822 Shawul AA, Chakma S (2019) Spatiotemporal detection of land use/land cover change in the large basin using  
823 integrated approaches of remote sensing and GIS in the Upper Awash basin, Ethiopia. *Environ Earth Sci*  
824 78:1–13. <https://doi.org/10.1007/s12665-019-8154-y>
- 825 Shawul AA, Chakma S, Melesse AM (2019) The response of water balance components to land cover change  
826 based on hydrologic modeling and partial least squares regression (PLSR) analysis in the Upper Awash  
827 Basin. *J Hydrol Reg Stud* 26:100640. <https://doi.org/10.1016/j.ejrh.2019.100640>
- 828 Tabari H (2020) Climate change impact on flood and extreme precipitation increases with water availability. *Sci*  
829 *Rep* 10:1–10. <https://doi.org/10.1038/s41598-020-70816-2>
- 830 Tadese M, Kumar L, Koech R (2020a) Long-term variability in potential evapotranspiration, water availability  
831 and drought under climate change scenarios in the Awash River Basin, Ethiopia. *Atmosphere (Basel)* 11:.  
832 <https://doi.org/10.3390/ATMOS11090883>
- 833 Tadese M, Kumar L, Koech R, Kogo BK (2020b) Mapping of land-use/land-cover changes and its dynamics in  
834 Awash River Basin using remote sensing and GIS. *Remote Sens Appl Soc Environ* 19:100352.  
835 <https://doi.org/10.1016/j.rsase.2020.100352>
- 836 Tadese MT, Kumar L, Koech R, Zemadim B (2019) Hydro-climatic variability: A characterisation and trend  
837 study of the Awash River Basin, Ethiopia. *Hydrology* 6: . <https://doi.org/10.3390/hydrology6020035>
- 838 Taye MT, Dyer E, Hirpa FA, Charles K (2018) Climate change impact on water resources in the Awash basin,  
839 Ethiopia. *Water (Switzerland)* 10:1–16. <https://doi.org/10.3390/w10111560>
- 840 Tekleab S, Mohamed Y, Uhlenbrook S (2013) Hydro-climatic trends in the Abay/Upper Blue Nile basin,  
841 Ethiopia. *Phys Chem Earth* 61–62:32–42. <https://doi.org/10.1016/j.pce.2013.04.017>
- 842 Theil H (1950) A rank-invariant method of linear and polynomial regression analysis. *Proc K Ned Akad van*  
843 *Wet Series A* 5:386–392
- 844 Tigabu TB, Hörmann G, Wagner PD, Fohrer N (2020) Statistical analysis of rainfall and streamflow time series  
845 in the Lake Tana Basin, Ethiopia. *J Water Clim Chang* 11:258–273. <https://doi.org/10.2166/wcc.2018.008>
- 846 Vandana K, Islam A, Sarthi PP, et al (2019) Assessment of potential impact of climate change on streamflow: A  
847 case study of the brahmani river basin, India. *J Water Clim Chang* 10:624–641.  
848 <https://doi.org/10.2166/wcc.2018.129>
- 849 Von Storch H, Navarra A (1995) *Analysis of Climate Variability*. Springer-Verlag, New York
- 850 Wagesho N, Goel NK, Jain MK (2012) Investigation of non-stationarity in hydro-climatic variables at Rift  
851 Valley lakes basin of Ethiopia. *J Hydrol* 444–445:113–133. <https://doi.org/10.1016/j.jhydrol.2012.04.011>
- 852 WaleWorqlul A, Taddele YD, Ayana EK, et al (2018) Impact of climate change on streamflow hydrology in  
853 headwater catchments of the upper Blue Nile Basin, Ethiopia. *Water (Switzerland)* 10:.  
854 <https://doi.org/10.3390/w10020120>
- 855 Wang W, Chen Y, Becker S, Liu B (2015) Linear trend detection in serially dependent hydrometeorological  
856 data based on a variance correction Spearman rho method. *Water (Switzerland)* 7:7045–7065.  
857 <https://doi.org/10.3390/w7126673>
- 858 Wang Y, Xu Y, Tabari H, et al (2020) Innovative trend analysis of annual and seasonal rainfall in the Yangtze  
859 River Delta, eastern China. *Atmos Res* 231:104673. <https://doi.org/10.1016/j.atmosres.2019.104673>
- 860 Wasko C, Nathan R (2019) Influence of changes in rainfall and soil moisture on trends in flooding. *J Hydrol*  
861 575:432–441. <https://doi.org/10.1016/j.jhydrol.2019.05.054>

- 862 Williams LJ, Abdi H (2010) Tukey 's Honestly Signiflcant Difference test (HSD). *Encycl Res Des* 2–7
- 863 Wilson D, Hisdal H, Lawrence D (2010) Has streamflow changed in the Nordic countries? - Recent trends and  
864 comparisons to hydrological projections. *J Hydrol* 394:334–346.  
865 <https://doi.org/10.1016/j.jhydrol.2010.09.010>
- 866 Wu H, Qian H (2017) Innovative trend analysis of annual and seasonal rainfall and extreme values in Shaanxi,  
867 China, since the 1950s. *Int J Climatol* 37:2582–2592. <https://doi.org/10.1002/joc.4866>
- 868 Yue S, Wang C (2004) The Mann-Kendall Test Modified by Effective Sample Size to Detect Trend in Serially  
869 Correlated Hydrological Series. *Water Resour Manag* 18:201–218.  
870 <https://doi.org/10.1023/B:WARM.0000043140.61082.60>
- 871 Zena K, Adugna T, Fufa F (2020) Trend Analysis of Climate variables, Stream flow and their Linkage at Modjo  
872 River Watershed, Central Ethiopia. <https://doi.org/10.21203/rs.3.rs-16796/v1>
- 873 Zhou Z, Wang L, Lin A, et al (2018) Innovative trend analysis of solar radiation in China during 1962–2015.  
874 *Renew Energy* 119:675–689. <https://doi.org/10.1016/j.renene.2017.12.052>
- 875

## Supplementary Files

This is a list of supplementary files associated with this preprint. Click to download.

- [watershed.rar](#)